Cell Reports



# Pericytes Stimulate Oligodendrocyte Progenitor Cell Differentiation during CNS Remyelination

## Graphical Abstract

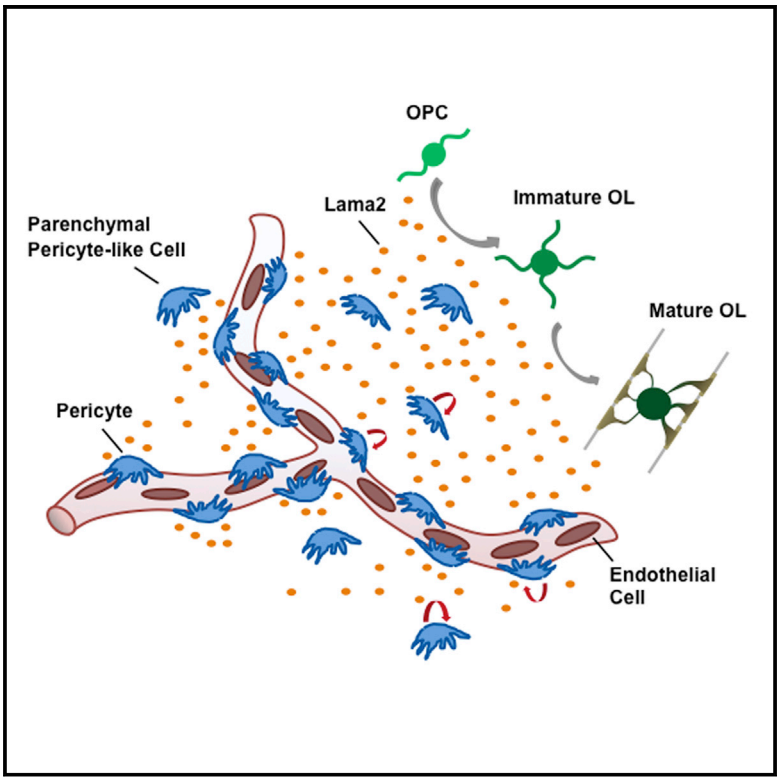


## Authors

Alerie Guzman De La Fuente, Simona Lange, Maria Elena Silva, ..., Ludwig Aigner, Robin J.M. Franklin, Francisco J. Rivera

## Correspondence

francisco.rivera@uach.cl

## In Brief

Following toxin-induced demyelination in PC-deficient mice and using a number of in vitro approaches, Guzman de la Fuente et al. show that CNS pericytes (PCs) respond to demyelination and, through Lama2 secretion, stimulate oligodendrocyte progenitor cell differentiation during remyelination. These findings extend PC function beyond vascular homeostasis toward regeneration.

## Highlights

- CNS-resident PCs react to demyelination and are found close to differentiating OPCs
- PC-deficient mice show delayed OPC differentiation during CNS remyelination
- PC-conditioned medium accelerates OPC differentiation and enhances remyelination
- PC-derived LAMA2 induces OPC differentiation

De La Fuente et al., 2017, Cell Reports *20*, 1755–1764
August 22, 2017 
http://dx.doi.org/10.1016/j.celrep.2017.08.007

Cell Reports
Report



# Pericytes Stimulate Oligodendrocyte Progenitor Cell Differentiation during CNS Remyelination

Alerie Guzman De La Fuente,[1,17] Simona Lange,[2,3,17] Maria Elena Silva,[1,2,3,4,5,6] Ginez A. Gonzalez,[1] Herbert Tempfer,[3,7,8] Peter van Wijngaarden,[1,9] Chao Zhao,[1] Ludovica Di Canio,[1] Andrea Trost,[2,3,10] Lara Bieler,[3,11] Pia Zaunmair,[3,11] Peter Rotheneichner,[3,11] Anna O'Sullivan,[3,11] Sebastien Couillard-Despres,[3,11] Oihana Errea,[1] Maarja A. Mäe,[12] Johanna Andrae,[12] Liqun He,[13] Annika Keller,[14] Luis F. Bátiz,[4,15] Christer Betsholtz,[12,16] Ludwig Aigner,[2,3,8,18] Robin J.M. Franklin,[1,18] and Francisco J. Rivera[1,2,3,4,5,18,19,*]

[1]Wellcome Trust and MRC Cambridge Stem Cell Institute, University of Cambridge, Cambridge CB20AH, UK
[2]Institute of Molecular Regenerative Medicine, Paracelsus Medical University Salzburg, 5020 Salzburg, Austria
[3]Spinal Cord Injury and Tissue Regeneration Center Salzburg (SCI-TReCS), Paracelsus Medical University Salzburg, 5020 Salzburg, Austria
[4]Laboratory of Stem Cells and Neuroregeneration, Institute of Anatomy, Histology and Pathology, Faculty of Medicine, Universidad Austral de Chile, Valdivia, Chile
[5]Center for Interdisciplinary Studies on the Nervous System (CISNe), Universidad Austral de Chile, Valdivia, Chile
[6]Institute of Pharmacy, Faculty of Sciences, Universidad Austral de Chile, Valdivia, Chile
[7]Institute for Tendon and Bone Regeneration, Paracelsus Medical University Salzburg, 5020 Salzburg, Austria
[8]Austrian Cluster for Tissue Regeneration, Vienna, Austria
[9]Centre for Eye Research Australia, Royal Victorian Eye and Ear Hospital, Ophthalmology, Department of Surgery, University of Melbourne, Australia
[10]Ophthalmology/Optometry and Research Program for Experimental Ophthalmology, Paracelsus Medical University Salzburg, 5020 Salzburg, Austria
[11]Institute of Experimental Neuroregeneration, Paracelsus Medical University Salzburg, 5020 Salzburg, Austria
[12]Department of Immunology, Genetics and Pathology, Rudbeck Laboratory, Uppsala University, 751 85 Uppsala, Sweden
[13]Department of Neurosurgery, Tianjin Medical University General Hospital, Tianjin Neurological Institute, Key Laboratory of Post-Neuroinjury Neuro-Repair and Regeneration in Central Nervous System, Ministry of Education and Tianjin City, Tianjin 300052, China
[14]Division of Neurosurgery, Zürich University Hospital, Zürich University, 8091 Zürich, Switzerland
[15]Centro de Investigación Biomédica (CIB), Facultad de Medicina, Universidad de los Andes, Santiago, Chile
[16]Integrated Cardio Metabolic Center (ICMC), Karolinska Institutet Novum, 141 57 Huddinge, Sweden
[17]These authors contributed equally
[18]Senior author
[19]Lead Contact
*Correspondence: francisco.rivera@uach.cl
http://dx.doi.org/10.1016/j.celrep.2017.08.007

## SUMMARY

**The role of the neurovascular niche in CNS myelin regeneration is incompletely understood. Here, we show that, upon demyelination, CNS-resident pericytes (PCs) proliferate, and parenchymal non-vessel-associated PC-like cells (PLCs) rapidly develop. During remyelination, mature oligodendrocytes were found in close proximity to PCs. In *Pdgfb*$^{ret/ret}$ mice, which have reduced PC numbers, oligodendrocyte progenitor cell (OPC) differentiation was delayed, although remyelination proceeded to completion. PC-conditioned medium accelerated and enhanced OPC differentiation in vitro and increased the rate of remyelination in an ex vivo cerebellar slice model of demyelination. We identified Lama2 as a PC-derived factor that promotes OPC differentiation. Thus, the functional role of PCs is not restricted to vascular homeostasis but includes the modulation of adult CNS progenitor cells involved in regeneration.**

## INTRODUCTION

Although the adult mammalian CNS has a limited capacity for regeneration, lost oligodendrocytes and the myelin they produce are restored during remyelination. In response to demyelination, oligodendrocyte progenitor cells (OPCs) proliferate and migrate to the lesion, where they differentiate into remyelinating oligodendrocytes (Franklin and Ffrench-Constant, 2008; Zawadzka et al., 2010). Remyelination restores saltatory conduction and ensures axonal survival, and its impairment renders demyelinated axons vulnerable to irreversible degeneration (Franklin et al., 2012). Thus, promoting remyelination is a major therapeutic objective in chronic demyelinating diseases such as multiple sclerosis, where remyelination becomes increasingly inefficient with disease progression (Goldschmidt et al., 2009).

Myelination during development is strictly coupled to angiogenesis (Yuen et al., 2014), where OPCs use the vasculature as scaffolds for migration (Tsai et al., 2016). Similarly, regeneration in the CNS is coupled to the vascular niche (Manavski et al., 2014). The CNS vascular niche consists of endothelial cells (ECs), vasculature-associated cells such as perivascular cells, astrocytes, neurons, OPCs, molecules derived from these cells, and blood-derived elements. Pericytes (PCs), which are located

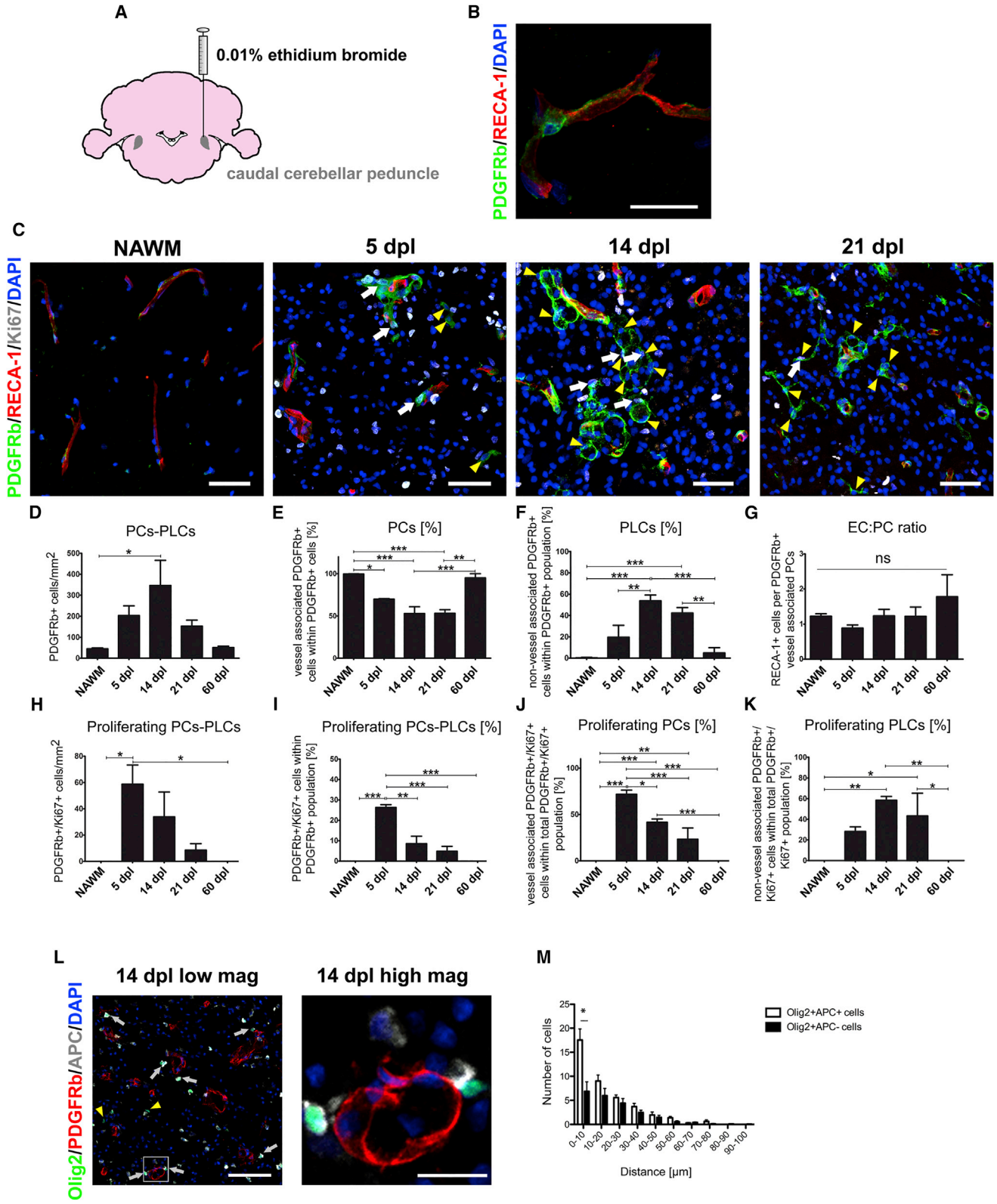


**Figure 1. Pericytes React to Demyelination**

(A) Ethidium bromide-induced demyelinated lesion in the CCP of adult rats.

(B) PDGFRb expressing PC and RECA-1+ ECs in NAWM.

*(legend continued on next page)*

at the abluminal surface of capillaries and embedded within the basement membrane, regulate angiogenesis and neovascularization and control microvascular blood flow (Armulik et al., 2010). The CNS contains the highest PC density in the body, ensuring proper blood-brain barrier (BBB) structure and function (Armulik et al., 2010; Winkler et al., 2011). CNS-resident PCs also share features with mesenchymal stem cells (MSCs), expressing similar genes and differentiating into cells of the mesenchymal lineage in vitro (Crisan et al., 2008). MSCs secrete a plethora of paracrine signaling molecules (Chen et al., 2009), including factors that promote oligodendrocyte differentiation (Jadasz et al., 2013; Rivera et al., 2006). We hypothesized that PCs act in a similar fashion (Lange et al., 2013). This assumption is supported by the close physical proximity between PCs and OPCs in healthy cerebral white matter (Maki et al., 2015) and by the ability of PC-derived transforming growth factor β 1 to regulate OPC migration during cortical development (Choe et al., 2014). Here we analyzed PCs, their response to a demyelinating lesion, and their functional role in oligodendrocyte differentiation during remyelination. In vivo relevance was studied through a genetic mouse model with reduced pericyte coverage. Moreover, molecular and cellular analysis identified the PC-derived factor modulating OPC differentiation.

## RESULTS

### Pericytes Respond to CNS Demyelination

We first analyzed the proliferative response and localization of ECs and PCs following induction of white matter demyelination upon injection of ethidium bromide into the caudal cerebellar peduncles (CCPs) of adult rats (Figure 1A). In this model, demyelination occurs within 24 hr of injection and induces OPC proliferation and migration, which peaks at 5 days post-lesion induction (dpl), followed by OPC differentiation, which is ongoing at 14 dpl. Remyelination is completed by 21 dpl. There was a significant increase in proliferating (Ki67-positive) rat endothelial cell antigen 1 (RECA-1)-expressing ECs and a robust proliferative response of platelet-derived growth factor receptor beta (PDGFRb)-expressing PCs within the demyelinated lesion at 5 dpl (Figures S1C and S1D), although the vessel area was not altered between 5 and 21 dpl (Figures S1A and S1B). In the normal-appearing white matter (NAWM), PCs are restricted to the perivascular region (Figure 1B). The total number of PDGFRb+ cells within the lesion was significantly increased at 14 dpl compared with NAWM (Figures 1C and 1D). This was accompanied by the appearance of PDGFRb+ cells away from blood vessels, which, because we cannot be certain of their origin, we defined as pericyte-like cells (PLCs) to distinguish them from PCs close to blood vessels (Figure 1C). Within the whole PDGFRb+ population (i.e., PCs and PLCs), the proportion of PCs declined during remyelination (Figure 1E), whereas the percentage of parenchymal PLCs increased and was highest at 14 dpl (Figure 1F). Consistent with the unaltered density of ECs and PCs during remyelination (Figures S1E and S1F), the EC:PC ratio, crucial for BBB stability (Armulik et al., 2010), remained the same (Figure 1G). At 5 dpl, there were numerous Ki67+ PDGFRb+ cells in the lesion that peaked at 14 dpl but declined thereafter and were absent at 60 dpl (Figures 1H–1K). By 60 dpl, when the lesion is fully remyelinated, PDGFRb+ cell numbers and localization were similar to that in NAWM, where only PCs and no PLCs were found (Figures 1C–1G). Staining for desmin, another PC marker, supported these findings (Figure S4A).

We hypothesized that, if PCs and/or PLCs were involved in the differentiation of OPCs into remyelinating oligodendrocytes, then the differentiated cells would tend to be located in close proximity to PDGFRb+ cells. We therefore assessed the distance between Olig2+/adenomatous polyposis coli (APC)− OPCs and Olig2+/APC+ oligodendrocytes to the nearest PDGFRb+ cell at 14 dpl. We found that oligodendrocytes were preferentially located close (i.e., within 10 μm) to PCs, whereas OPCs showed no preferential clustering close to these cells; neither was there clustering of either OPCs or oligodendrocytes close to PLCs (Figures 1L and 1M; Figures S1G and S1H). These results suggest that PCs and PLCs may have differential roles in modulating OPC function during remyelination.

### Impaired Oligodendrocyte Differentiation during Remyelination in PC-Deficient Mice

To determine whether CNS-resident PCs influence remyelination, we used *Pdgfb*$^{ret/ret}$ mice, in which a mutation in the retention motif of the *Pdgfb* gene causes a 75%–85% reduction in capillary PC coverage compared with heterozygous littermates (Figure 2A; Armulik et al., 2010; Lindblom et al., 2003). PDGFRb is still expressed in these mice and can still be used as a marker for residual pericytes.

We first examined myelination in *Pdgfb*$^{ret/ret}$ mice and found that, on post-natal day 12 (P12), the density of mature oligodendrocytes (Olig2+/APC+) was lower and the density of OPCs (Olig2+/APC−) higher than in control mice. However, on P17, no differences were observed in OPC differentiation and myelination (Figure S2).

Following lysolecithin-induced demyelination in the ventral spinal cord white matter (WM), the number of PDGFRb+ increased substantially in both *Pdgfb*$^{ret/ret}$ and control mice. The number of PDGFRb+ cells in *Pdgfb*$^{ret/ret}$ mice at 5 dpl was less than in control mice, and there were fewer PLCs. However,

(C) Proliferating PDGFRb+ cells and ECs (PDGFRb/RECA-1/Ki67) within lesions at 5, 14, and 21 dpl. White arrows indicate proliferating PCs and yellow arrowheads PLCs.

(D–K) Quantitative analyses of different PC parameters in response to demyelination.

(L) Immunohistochemistry showing the distance of OPCs (Olig2+/APC−), mature oligodendrocytes (Olig2+/APC+), and PDGFRb+ at 14 dpl; yellow arrowheads indicate OPCs and white arrows mature oligodendrocytes. The high-magnification image shows mature oligodendrocytes close to PDGFRb+ cells.

(M) The graph displays the distance distribution of OPCs and mature oligodendrocytes from PDGFRb + cells.

(C–M) 3 or more animals were analyzed for each time point.

(L and M) 150 or more distance measurements were performed from oligodendrocytes to PDGFRb+ cells per animal.

Means ± SEM are shown. Data were analyzed by one-way ANOVA followed by Tukey's post hoc test, Student's t test, or chi-square test. *$p < 0.05$, **$p < 0.01$, ***$p < 0.001$. Scale bars, (B) 20 μm; (C) 50 μm; (D) 50 μm, high-magnification 10 μm; (E) 50 μm, high magnification 10 μm.

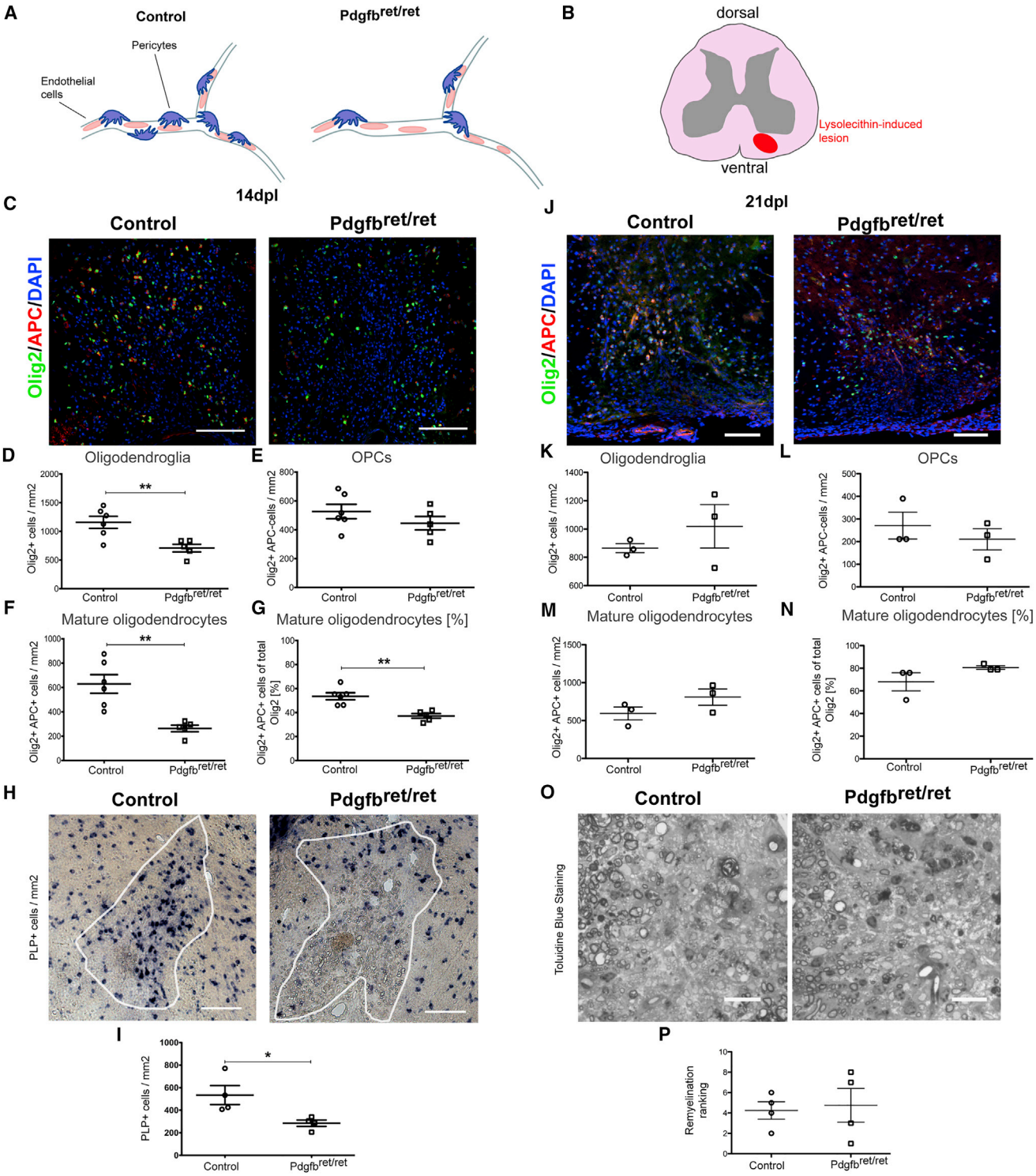


**Figure 2. OPC Differentiation Is affected during Remyelination in *Pdgfb*$^{ret/ret}$ Mice**

(A and B) Illustrations of decreased PC coverage in *Pdgfb*$^{ret/ret}$ mice (A) and of lysolecithin-induced demyelination (B).

(C and J) Mature oligodendrocytes (Olig2+/APC+) and OPCs (Olig2+/APC−) in lesions of control and *Pdgfb*$^{ret/ret}$ mice at 14 dpl (C) and 21dpl (J).

(D–G and K–N) Quantitative analyses of oligodendroglia at 14 dpl (D–G) and 21 dpl (K–N).

(H and I) In situ hybridization and quantification for PLP of control and *Pdgfb*$^{ret/ret}$ mice at 14 dpl.

(O and P) Toluidine blue staining of remyelination in control and *Pdgfb*$^{ret/ret}$ mice at 21 dpl (O) and its quantification by relative ranking analysis (P).

Means ± SEM are shown. Data were analyzed by Student's t test or Mann-Whitney *U* test. *p < 0.05, **p < 0.01, ***p < 0.001. Scale bars, 100 μm.

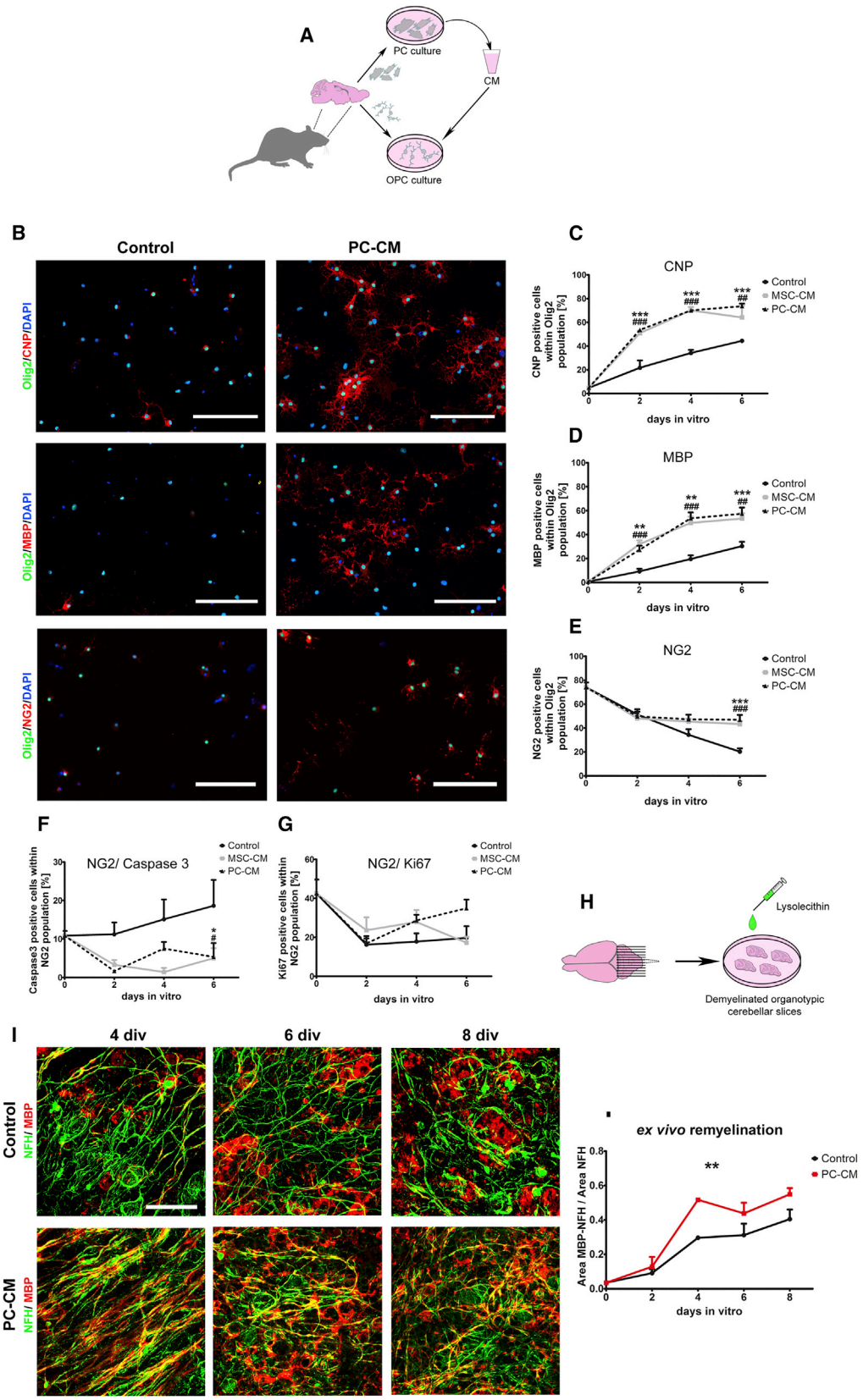


*(legend on next page)*

by 14 dpl, the density of PDGFRb+ cells was the same in both groups because of a higher proliferative response of these cells in the *Pdgfb*$^{ret/ret}$ mice (Figures S3A–S3F). No differences were detected in the astrocyte or in the macrophage/microglial response between *Pdgfb*$^{ret/ret}$ mice and control mice (Figures S3G–S3I). Microglia/macrophages showed the same pro-inflammatory and anti-inflammatory cell profile distribution in both groups (Figures S3J–S3L), and no differences were detected in BBB stability in the lesion area (Figures S3M–S3Q).

The total number of Olig2+ cells within the lesion was reduced in *Pdgfb*$^{ret/ret}$ mice compared with controls at 14 dpl. There was no significant difference in the number of Olig2+/APC− OPCs between *Pdgfb*$^{ret/ret}$ and control mice (Figures 2C and 2E). However, the number of Olig2+/APC+ mature oligodendrocytes was significantly reduced in *Pdgfb*$^{ret/ret}$mice (Figures 2C, 2F, and 2G). In situ hybridization for proteolipid protein (PLP), a major myelin component, generated consistent results (Figures 2H and 2I). However, the densities of Olig2+ cells and Olig2+APC+ oligodendrocytes were the same in both groups by 21 dpl (Figures 2J–2N). No differences were detected in the extent of remyelination, as assessed by ranking analysis of toluidine blue-stained resin sections in which demyelinated and remyelinated axons were discernable (Figures 2O and 2P).

These data indicate that *Pdgfb*$^{ret/ret}$ mice show a delay in OPC differentiation because of the decreased numbers of PDGFRb+ cells at the earlier stages following demyelination. However, because the PDGFRb+ cell numbers normalize by 14 dpl, this delay does not translate into a decrease in remyelination.

## PCs Promote OPC Differentiation and Enhance Remyelination Ex Vivo

We next examined how PCs might directly influence OPC function. We therefore exposed cultured OPCs to PC-conditioned medium (PC-CM) and evaluated the rate of differentiation. MSC-conditioned medium (MSC-CM), previously identified as a strong inducer of OPC differentiation (Jadasz et al., 2013), was used as a positive control. Primary PCs exhibiting MSCs features, including mesenchymal differentiation potential, were isolated from adult rat brains (Figure 3A; Figures S4B–S4D). Upon incubation with PC-CM, a higher proportion of OPCs had acquired 2′,3′-cyclic-nucleotide 3′-phosphodiesterase (CNP) and myelin basic protein (MBP) expression at 2 days in vitro (DIV) compared with those exposed to non-conditioned control medium (Figures 3B–3D). We also found a significantly higher proportion of NG2+/Olig2+ OPCs in the PC-CM-treated cultures (Figures 3B and 3E). This effect was likely due to an anti-apoptotic effect of the PC-CM because PC-CM significantly decreased the proportion of caspase-3-positive OPCs compared with control conditions (Figure 3F). Proliferation, assessed by Ki67 staining, was not affected by PC-CM (Figure 3G).

We next examined whether PCs can enhance remyelination. We used postnatal rat-derived cerebellar organotypic slice cultures as an ex vivo model of remyelination (Yuen et al., 2013; Zhang et al., 2011). In this model, P10 rat cerebellar slices were demyelinated using lysolecithin (Birgbauer et al., 2004) and then exposed to PC-CM or control medium (Figure 3H). Remyelination was analyzed at 0, 2, 4, 6, and 8 days after lysolecithin treatment by immunohistochemical staining for MBP and neurofilament heavy chain (NFH). PC-CM significantly enhanced the remyelination rate after lysolecithin-induced demyelination (Figures 3I and 3J).

## PC-Induced OPC Differentiation Is Mediated through Lama2

We have previously shown that Lama2 mRNA expression is decreased in the microvessels of *Pdgfb*$^{ret/ret}$ mice compared with control mice (Armulik et al., 2010; Figure 4B). The *Lama2* gene product is highly expressed during remyelination (Zhao et al., 2009) and has been shown to modulate OPC function (Relucio et al., 2012). Given that the main source of Lama2 within the microvessels is PDGFRb+ cells, as shown by RNA sequencing (RNA-seq) (He et al., 2016; Figure 4A), we investigated whether Lama2 is a mediator of the PC-induced effect on OPC differentiation. RNA in situ hybridization of healthy brain sections revealed a specific expression of Lama2 in cells expressing the PC markers PDGFRb and CD13 (Figure 4D). In control mice, Lama2 was mainly detected around cell bodies and processes of PCs, whereas *Pdgfb*$^{ret/ret}$ mice had less Lama2 protein expression that, when present, was always associated with residual PCs (Figure 4E). Cultured PCs also expressed Lama2 (Figure 4C). Pre-incubation of PC-CM with an anti-Lama2 antibody resulted in a significant decrease in the Olig2+/CNP+ and Olig2+/MBP+ populations compared with PC-CM pre-incubated with a general immunoglobulin G (IgG), reducing OPC differentiation to a level indistinguishable from control conditions (Figures 4F and 4G). These results were replicated in OPCs exposed to PC-CM harvested from PCs treated with either non-targeting or Lama2 small interfering RNA (siRNA) for 48 hr (Figures 4H and 4I). Taken together, these data identify Lama2 as a PC-derived molecule that promotes OPC differentiation.

## DISCUSSION

This work reveals an unidentified role of PCs in CNS regeneration. We show that PCs in the vessel walls respond to

**Figure 3. PCs Promote OPC Differentiation and Accelerate Remyelination in Demyelinated Organotypic Slices**

(A) Schematic of the experimental design.

(B–E) Fluorescence images (B) displaying CNP+/Olig2+, MBP+/Olig2+, and NG2+/Olig2+ oligodendrocytes at 4 DIV and their respective graphs (C–E).

(F and G) PC-CM increases the generation of oligodendrocytes from OPCs. Graphs display (F) the OPC survival rate (NG2+/Caspase+) and (G) the OPC proliferation rate (NG2+/Ki67+) under different conditions.

(H) Illustration of lysolecithin-induced demyelination of slice cultures.

(I) Images showing axons (NFH+) and myelin (MBP+) of remyelinating cerebellar slices exposed to control medium versus PC-CM at 4, 6, and 8 days post lysolecithin treatment.

(J) Quantification of the MBP/NFH ratio shows that PC-CM increases the remyelination rate. 3 or more independent OPC and slice preparations were used. Means ± SEM are shown. Data were analyzed by two-way ANOVA followed by Bonferroni's post hoc test. *$p < 0.05$, **$p < 0.01$, ***$p < 0.001$. * indicates statistical difference for PC-CM and # for MSC-CM. Scale bars, (B) 100 μm and (I) 50 μm.

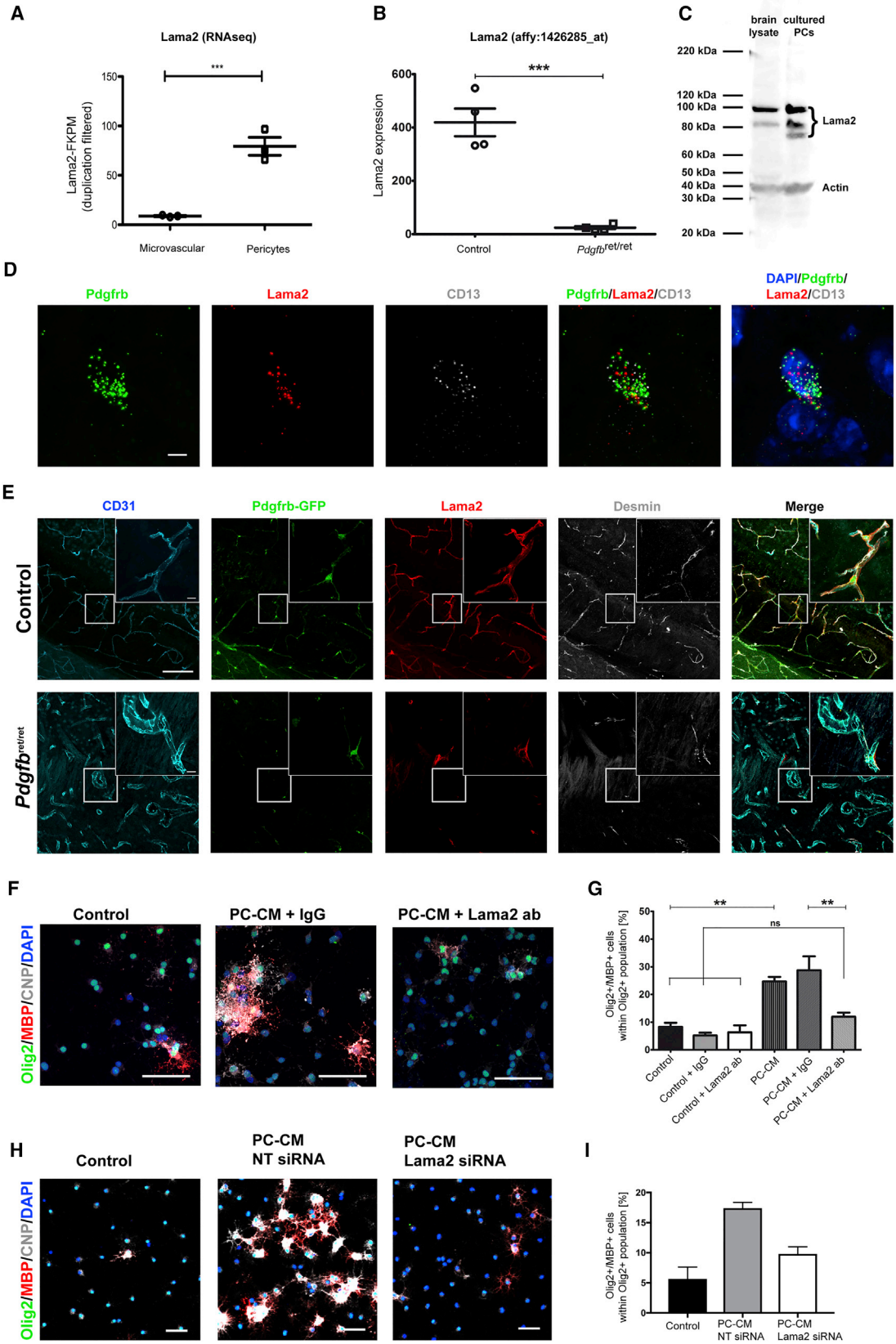


*(legend on next page)*

demyelination by proliferation. We describe a parenchymal cell population expressing PC markers such as PDGFRb and desmin that appears soon after the induction of demyelination. Although these cells express PC markers, we cannot be certain of their origin, and, therefore, we refer to them as PLCs. Upon demyelination, both PCs and PLCs have a high proliferative response; however, mature oligodendrocytes are preferentially located in higher frequency close to PCs. These data suggest that, even though both populations respond to demyelination, they may have differential roles in their interaction with OPCs during remyelination, which will require further investigation. In mice with a reduced PC density, OPC differentiation is delayed in the demyelinated lesion, resulting in fewer mature oligodendrocytes at 14 dpl. Moreover, exposure to PC-CM accelerated OPC differentiation and enhanced ex vivo remyelination. We identified Lama2 as a key factor responsible for the effect of PCs in promoting OPC differentiation.

In humans, loss of *LAMA2* gene expression causes WM abnormalities, manifested at an early postnatal age, when developmental myelination occurs (Allamand and Guicheney, 2002). Similarly, a mouse model for Lama2 deficiency (*Lama2*$^{-/-}$) shows developmental delays in oligodendrocyte differentiation and the accumulation of OPCs, leading to defects in myelination in the corpus callosum (Chun et al., 2003; Relucio et al., 2012). Lama2 regulates OPC function through its interaction with dystroglycan (Leiton et al., 2015). In the CNS, Lama2 is expressed by PCs and upregulated during OPC differentiation (14 dpl) in a toxin-induced demyelination model (Zhao et al., 2009). Lama2 seems to be relevant for PC function because *Lama2*$^{-/-}$ mice have decreased microvascular PC coverage associated with BBB defects (Menezes et al., 2014). Our data suggest that PC-derived Lama2 has a key role in promoting OPC differentiation because the PC-CM effect in OPCs was inhibited when exposed to an anti-Lama2 antibody or when PCs were treated with Lama2 siRNA. Consistent with this, we observed that OPC differentiation was delayed in adult *Pdgfb*$^{ret/ret}$ mice after lysolecithin-induced demyelination. These findings indicate that PCs provide an appropriate milieu for differentiating OPCs through Lama2.

This study indicates that PC functions are not restricted to vascular homeostasis but, rather, extend to CNS regeneration. This is supported by studies illustrating that PCs respond with high proliferation to acute lesions such as stroke or spinal cord injury (SCI), where they modulate inflammation or the formation of fibrotic scar tissue (Göritz et al., 2011; Özen et al., 2014). Here we show that, besides stabilizing CNS vasculature and regulating EC function, pericytes also have a high proliferative response following CNS demyelination and directly influence CNS-resident progenitor cell differentiation during remyelination, most likely by secretion of Lama2.

## EXPERIMENTAL PROCEDURES

### Animal Work

Animal experiments within this research have been regulated under the Animals (Scientific Procedures) Act 1986 Amendment Regulations 2012 following ethical review by the University of Cambridge Animal Welfare and Ethical Review Body (AWERB) in accordance with United Kingdom Home Office regulations (Project License 70/7715) and in accordance with Austrian laws on animal experimentation and were approved by Austrian regulatory authorities (Permit No. BMWF-66.012/0001-II/3b/2014; license codes BMBF-66-012/0037-WF/V/3b/2014 and BMWF-66.012/0032-WF/V/3b/2015). During this study, 2- to 3-month-old Sprague Dawley rats and 12-week-old *Pdgfb*ret/ret mice (hetero- and homozygous), which were previously described by Armulik et al. (2010) and Lindblom et al. (2003), were used for toxin-induced demyelination.

### Cell Culture

Preparation of CNS pericytes was performed following the Dore-Duffy protocol (Dore-Duffy et al., 2006) with modifications. Rat bone marrow-derived MSCs were prepared as described previously by Rivera et al. (2006). OPCs were prepared from neonatal P0–P2 Sprague-Dawley rats, cortices and hippocampi were digested with papain solution, and dissociated cells were seeded into poly-D-lysine-coated T75 flasks. Mixed glial cultures were kept for 11 DIV in medium with DMEM (Gibco) and 10% fetal bovine serum (Biosera). OPCs were isolated as described previously (McCarthy and de Vellis, 1980).

### Organotypic Cerebellar Slices

Remyelination of rat cerebellar slices was prepared as described previously (Birgbauer et al., 2004). After 7 DIV, the medium was replaced with organotypic slice medium containing 0.5 mg/mL lysolecithin for 16 hr. After 16 hr, the medium was replaced with PC-conditioned organotypic slice medium and non-conditioned control medium.

### Statistical Analyses

Graphs show mean values ± SEM, and statistical analysis were performed using GraphPad Prism 5.0 (GraphPad) and SPSS 20 (IBM). Parametric one-way ANOVA, Tukey post hoc analyses, Student's t test, or Mann-Whitney *U* tests (when not normally distributed) were used when comparing one parameter. For statistical analysis with two parameters, such as time course experiments with different treatments, two-way ANOVA with Bonferroni post hoc was used. For distance frequency distribution analysis, chi-square test

**Figure 4. PC-Derived Lama2 Promotes OPC Differentiation and Is Decreased in *Pdgfb*$^{ret/ret}$ Mice**

(A) RNA-seq data showing the expression of Lama2 in the microvasculature (mainly consisting of a majority of ECs with very low PC contribution) versus sorted PCs (data extracted from He et al., 2016).

(B) Downregulation of Lama2 in microvessels of *Pdgfb*$^{ret/ret}$ mice (Affymetrix array data extracted from He et al., 2016).

(C) Western blot image indicating Lama2 expressed by PCs in vivo (brain) and in vitro.

(D) RNA in situ hybridization images showing PC-specific expression of PDGFRb, CD13, and Lama2.

(E) Confocal images of CD31/PDGFRb-GFP/Lama2/desmin of *Pdgfb*$^{ret/+}$ × *Pdgfrb*-EGFP mice compared with *Pdgfb*$^{ret/ret}$ × *Pdgfrb*-EGFP indicate PC-specific expression of Lama2 and show a decline of PCs and Lama2 in *Pdgfb*$^{ret/ret}$ mice. Boxed areas represent high-magnification images.

(F) Fluorescence images of oligodendrocytes (Olig2+/MBP+) 2 DIV with control medium, PC-CM with IgG, and PC-CM with anti-Lama2-blocking antibody.

(G) Graph displaying the percentage of Olig2+/MBP+ cells.

(H) Fluorescence images of OPCs in control medium, PC- CM from non-targeting siRNA, and PC Lama2 siRNA-treated-CM.

(I) Graph displaying the Olig2+/MBP+ cell population in the presence of the different siRNA-treated PC-CMs. n = 4 mice per group, and 3 or more independent cell preparations were used, except for siRNA experiments, where n = 2.

Means ± SEM are shown. Data were analyzed by Student's t test or one-way ANOVA followed by Tukey's post hoc test. *$p < 0.05$, **$p < 0.01$, ***$p < 0.001$. Scale bars, (C) 5 μm; (D) 100 μm, high-magnification 10 μm; (E) and (G), 50 μm.

was used (Figure 1M; Figures S1G and S1H). All experiments were performed as indicated by n in the figure legends. Significance was as follows: $p^* < 0.05$, $p^{**} < 0.01$, and $p^{***} < 0.001$.

For further details, see the Supplemental Experimental Procedures.

## SUPPLEMENTAL INFORMATION

Supplemental Information includes Supplemental Experimental Procedures and four figures and can be found with this article online at http://dx.doi.org/10.1016/j.celrep.2017.08.007.

## AUTHOR CONTRIBUTIONS

S.L. and F.J.R. conceived the project. A.G.D.L.F., S.L., L.A., R.J.M.F., and F.J.R. designed the study. S.L., A.G.D.L.F., L.F.B., C.B., L.A., R.J.M.F., and F.J.R. wrote and edited the manuscript. S.L. and A.G.D.L.F. designed the figures. A.G.D.L.F., S.L., H.T., C.Z., A.K., G.A.G., L.D.C., M.A.M., J.A., C.B., R.J.M.F., L.A., and F.J.R. planned the experiments. A.G.D.L.F., S.L., M.E.S., P.v.W., P.R., O.E., C.Z., G.A.G., A.K., M.A.M., J.A., and L.D.C. conducted the experiments. A.G.D.L.F., S.L., M.E.S., H.T., A.T., P.R., A.O., L.B., A.K., M.A.M., J.A., and F.J.R. collected data. A.G.D.L.F., S.L., M.E.S., G.A.G., L.D.C., C.Z., P.R., A.T., L.H., A.K., M.A.M., and J.A. analyzed data. A.G.D.L.F., S.L., P.R., G.A.G., A.K., M.A.M., J.A., C.B., R.J.M.F., L.A., and F.J.R. interpreted data. H.T., A.T., P.R., A.O., P.Z., S.C.D., and L.B. assisted technically. R.J.M.F., L.A., and F.J.R. supervised the project. C.B., L.A., R.J.M.F., and F.J.R. supported this study financially.

## ACKNOWLEDGMENTS

We thank Hannelore Bauer, Peter Hammerl, and Andreas Traweger for technical advice and support. This work was supported by research funds from Chilean FONDECYT Program CONICYT Grants 1161787 (to F.J.R.) and 1141015 (to L.F.B); Direccion de Investigación y Desarrollo-Universidad Austral de Chile (DID-UACh); Paracelsus Medical University PMU-FFF Long-Term Fellowship L-12/01/001-RIV (to F.J.R.) and Stand-Alone Grant E-12/15/077-RIT (to F.J.R. and A.T.); the European Union Seventh Framework Program (FP7/2007-2013) under Grant Agreements HEALTH-F2-2011-278850 (INMiND), HEALTH-F2-2011-279288 (IDEA), and FP7-REGPOT-316120 (GlowBrain); Austrian Science Fund FWF Special Research Program (SFB) F44 (F4413-B23) "Cell Signaling in Chronic CNS Disorders"; and State Government of Salzburg, Austria (Stiftungsprofessur and 20204-WISS/80/199-2014). In addition, this study was supported by grants from a core support grant from the Wellcome Trust (203151/Z/16/Z) and MRC to the Wellcome Trust–Medical Research Council Cambridge Stem Cell Institute, the UK Multiple Sclerosis Society (941/11), the David and Isobel Walker Trust, "Investissements d'avenir" IHU-A-ICM and Obra Social La Caixa, the Swedish Science Council (2015-00550), the Swedish Cancer Foundation (15 0735), the Knut and Alice Wallenberg Foundation (2015.0030), the European Research Council (AdG 294556 BBBARRIER), and the Leducq Foundation (Sphingonet; 14CVD02). P.v.W. was supported by National Health & Medical Research Council of Australia Early Career Fellowship 628928. Work in A.K.'s group was funded by the Swiss National Science Foundation (31003A_159514/1; http://www.snf.ch/en) and The Synapsis Foundation (http://www.alzheimer-synapsis.ch).

Received: May 9, 2016
Revised: May 6, 2017
Accepted: July 28, 2017
Published: August 22, 2017

## REFERENCES

Allamand, V., and Guicheney, P. (2002). Merosin-deficient congenital muscular dystrophy, autosomal recessive (MDC1A, MIM#156225, LAMA2 gene coding for alpha2 chain of laminin). Eur. J. Hum. Genet. *10*, 91–94.

Armulik, A., Genové, G., Mäe, M., Nisancioglu, M.H., Wallgard, E., Niaudet, C., He, L., Norlin, J., Lindblom, P., Strittmatter, K., et al. (2010). Pericytes regulate the blood-brain barrier. Nature *468*, 557–561.

Birgbauer, E., Rao, T.S., and Webb, M. (2004). Lysolecithin induces demyelination in vitro in a cerebellar slice culture system. J. Neurosci. Res. *78*, 157–166.

Chen, C.W., Montelatici, E., Crisan, M., Corselli, M., Huard, J., Lazzari, L., and Péault, B. (2009). Perivascular multi-lineage progenitor cells in human organs: regenerative units, cytokine sources or both? Cytokine Growth Factor Rev. *20*, 429–434.

Choe, Y., Huynh, T., and Pleasure, S.J. (2014). Migration of oligodendrocyte progenitor cells is controlled by transforming growth factor β family proteins during corticogenesis. J. Neurosci. *34*, 14973–14983.

Chun, S.J., Rasband, M.N., Sidman, R.L., Habib, A.A., and Vartanian, T. (2003). Integrin-linked kinase is required for laminin-2-induced oligodendrocyte cell spreading and CNS myelination. J. Cell Biol. *163*, 397–408.

Crisan, M., Yap, S., Casteilla, L., Chen, C.W., Corselli, M., Park, T.S., Andriolo, G., Sun, B., Zheng, B., Zhang, L., et al. (2008). A perivascular origin for mesenchymal stem cells in multiple human organs. Cell Stem Cell *3*, 301–313.

Dore-Duffy, P., Katychev, A., Wang, X., and Van Buren, E. (2006). CNS microvascular pericytes exhibit multipotential stem cell activity. J. Cereb. Blood Flow Metab. *26*, 613–624.

Franklin, R.J., and Ffrench-Constant, C. (2008). Remyelination in the CNS: from biology to therapy. Nat. Rev. Neurosci. *9*, 839–855.

Franklin, R.J., Ffrench-Constant, C., Edgar, J.M., and Smith, K.J. (2012). Neuroprotection and repair in multiple sclerosis. Nat. Rev. Neurol. *8*, 624–634.

Goldschmidt, T., Antel, J., König, F.B., Brück, W., and Kuhlmann, T. (2009). Remyelination capacity of the MS brain decreases with disease chronicity. Neurology *72*, 1914–1921.

Göritz, C., Dias, D.O., Tomilin, N., Barbacid, M., Shupliakov, O., and Frisén, J. (2011). A pericyte origin of spinal cord scar tissue. Science *333*, 238–242.

He, L., Vanlandewijck, M., Raschperger, E., Andaloussi Mäe, M., Jung, B., Lebouvier, T., Ando, K., Hofmann, J., Keller, A., and Betsholtz, C. (2016). Analysis of the brain mural cell transcriptome. Sci. Rep. *6*, 35108.

Jadasz, J.J., Kremer, D., Göttle, P., Tzekova, N., Domke, J., Rivera, F.J., Adjaye, J., Hartung, H.P., Aigner, L., and Küry, P. (2013). Mesenchymal stem cell conditioning promotes rat oligodendroglial cell maturation. PLoS ONE *8*, e71814.

Lange, S., Trost, A., Tempfer, H., Bauer, H.C., Bauer, H., Rohde, E., Reitsamer, H.A., Franklin, R.J., Aigner, L., and Rivera, F.J. (2013). Brain pericyte plasticity as a potential drug target in CNS repair. Drug Discov. Today *18*, 456–463.

Leiton, C.V., Aranmolate, A., Eyermann, C., Menezes, M.J., Escobar-Hoyos, L.F., Husain, S., Winder, S.J., and Colognato, H. (2015). Laminin promotes metalloproteinase-mediated dystroglycan processing to regulate oligodendrocyte progenitor cell proliferation. J. Neurochem. *135*, 522–538.

Lindblom, P., Gerhardt, H., Liebner, S., Abramsson, A., Enge, M., Hellstrom, M., Backstrom, G., Fredriksson, S., Landegren, U., Nystrom, H.C., et al. (2003). Endothelial PDGF-B retention is required for proper investment of pericytes in the microvessel wall. Genes Dev. *17*, 1835–1840.

Maki, T., Maeda, M., Uemura, M., Lo, E.K., Terasaki, Y., Liang, A.C., Shindo, A., Choi, Y.K., Taguchi, A., Matsuyama, T., et al. (2015). Potential interactions between pericytes and oligodendrocyte precursor cells in perivascular regions of cerebral white matter. Neurosci. Lett. *597*, 164–169.

Manavski, Y., Boon, R.A., and Dimmeler, S. (2014). Vascular niche controls organ regeneration. Circ. Res. *114*, 1077–1079.

McCarthy, K.D., and de Vellis, J. (1980). Preparation of separate astroglial and oligodendroglial cell cultures from rat cerebral tissue. J. Cell Biol. *85*, 890–902.

Menezes, M.J., McClenahan, F.K., Leiton, C.V., Aranmolate, A., Shan, X., and Colognato, H. (2014). The extracellular matrix protein laminin α2 regulates the maturation and function of the blood-brain barrier. J. Neurosci. *34*, 15260–15280.

Özen, I., Deierborg, T., Miharada, K., Padel, T., Englund, E., Genové, G., and Paul, G. (2014). Brain pericytes acquire a microglial phenotype after stroke. Acta Neuropathol. *128*, 381–396.

Relucio, J., Menezes, M.J., Miyagoe-Suzuki, Y., Takeda, S., and Colognato, H. (2012). Laminin regulates postnatal oligodendrocyte production by promoting oligodendrocyte progenitor survival in the subventricular zone. Glia *60*, 1451–1467.

Rivera, F.J., Couillard-Despres, S., Pedre, X., Ploetz, S., Caioni, M., Lois, C., Bogdahn, U., and Aigner, L. (2006). Mesenchymal stem cells instruct oligodendrogenic fate decision on adult neural stem cells. Stem Cells *24*, 2209–2219.

Tsai, H.H., Niu, J., Munji, R., Davalos, D., Chang, J., Zhang, H., Tien, A.C., Kuo, C.J., Chan, J.R., Daneman, R., and Fancy, S.P. (2016). Oligodendrocyte precursors migrate along vasculature in the developing nervous system. Science *351*, 379–384.

Winkler, E.A., Bell, R.D., and Zlokovic, B.V. (2011). Central nervous system pericytes in health and disease. Nat. Neurosci. *14*, 1398–1405.

Yuen, T.J., Johnson, K.R., Miron, V.E., Zhao, C., Quandt, J., Harrisingh, M.C., Swire, M., Williams, A., McFarland, H.F., Franklin, R.J., and Ffrench-Constant, C. (2013). Identification of endothelin 2 as an inflammatory factor that promotes central nervous system remyelination. Brain *136*, 1035–1047.

Yuen, T.J., Silbereis, J.C., Griveau, A., Chang, S.M., Daneman, R., Fancy, S.P., Zahed, H., Maltepe, E., and Rowitch, D.H. (2014). Oligodendrocyte-encoded HIF function couples postnatal myelination and white matter angiogenesis. Cell *158*, 383–396.

Zawadzka, M., Rivers, L.E., Fancy, S.P., Zhao, C., Tripathi, R., Jamen, F., Young, K., Goncharevich, A., Pohl, H., Rizzi, M., et al. (2010). CNS-resident glial progenitor/stem cells produce Schwann cells as well as oligodendrocytes during repair of CNS demyelination. Cell Stem Cell *6*, 578–590.

Zhang, H., Jarjour, A.A., Boyd, A., and Williams, A. (2011). Central nervous system remyelination in culture–a tool for multiple sclerosis research. Exp. Neurol. *230*, 138–148.

Zhao, C., Fancy, S.P., Franklin, R.J., and Ffrench-Constant, C. (2009). Up-regulation of oligodendrocyte precursor cell alphaV integrin and its extracellular ligands during central nervous system remyelination. J. Neurosci. Res. *87*, 3447–3455.

**Cell Reports, Volume *20***

## Supplemental Information

# Pericytes Stimulate Oligodendrocyte Progenitor Cell Differentiation during CNS Remyelination

**Alerie Guzman De La Fuente, Simona Lange, Maria Elena Silva, Ginez A. Gonzalez, Herbert Tempfer, Peter van Wijngaarden, Chao Zhao, Ludovica Di Canio, Andrea Trost, Lara Bieler, Pia Zaunmair, Peter Rotheneichner, Anna O'Sullivan, Sebastien Couillard-Despres, Oihana Errea, Maarja A. Mäe, Johanna Andrae, Liqun He, Annika Keller, Luis F. Bátiz, Christer Betsholtz, Ludwig Aigner, Robin J.M. Franklin, and Francisco J. Rivera**

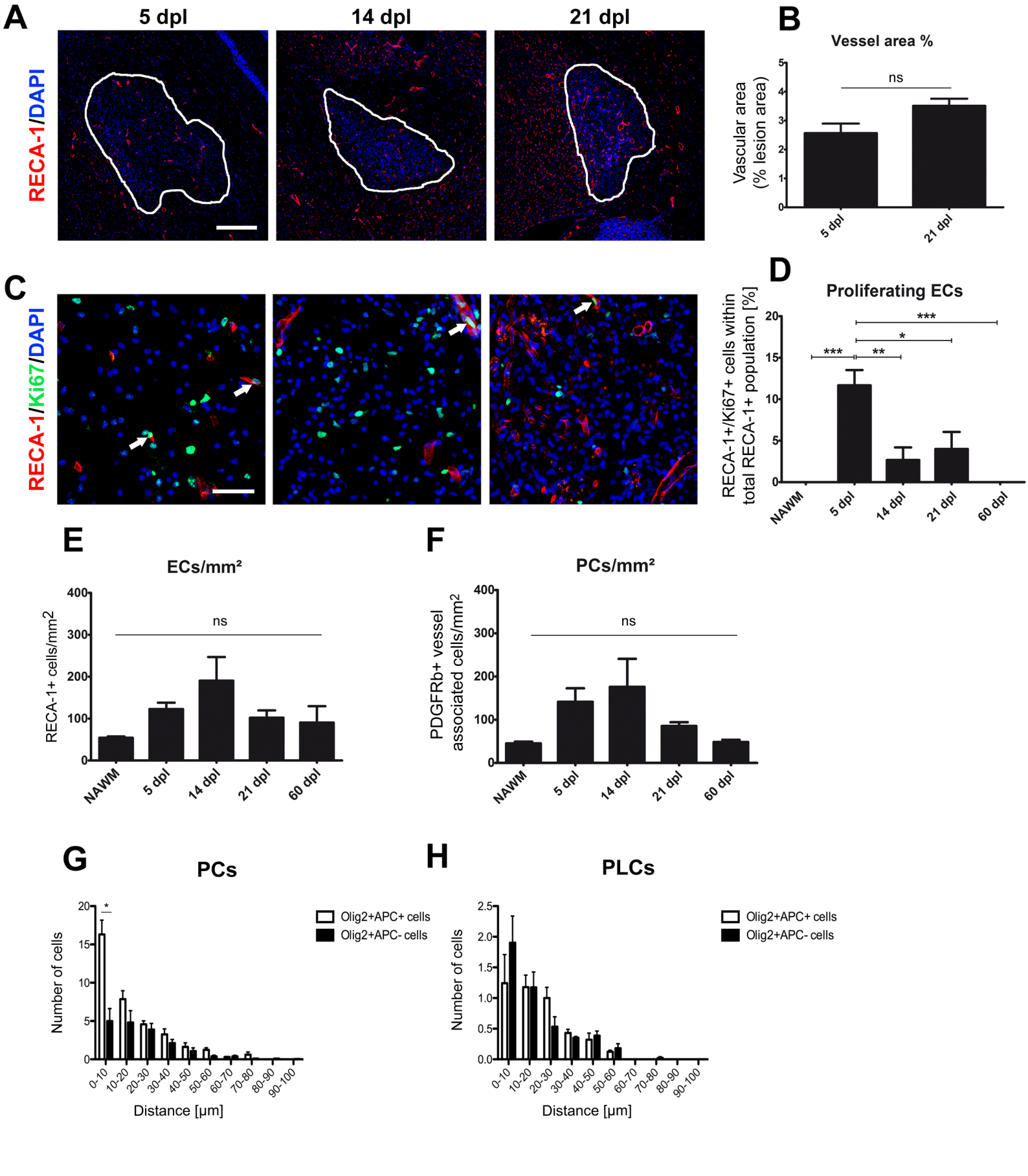
A
5 dpl
14 dpl
21 dpl
RECA-1/DAPI
B
Vessel area %
Vascular area (% lesion area)
ns
5 dpl
21 dpl
C
RECA-1/Ki67/DAPI
D
Proliferating ECs
RECA-1+/Ki67+ cells within total RECA-1+ population [%]
***
**
*
***
NAWM
5 dpl
14 dpl
21 dpl
60 dpl
E
ECs/mm²
RECA-1+ cells/mm2
ns
NAWM
5 dpl
14 dpl
21 dpl
60 dpl
F
PCs/mm²
PDGFRb+ vessel associated cells/mm2
ns
NAWM
5 dpl
14 dpl
21 dpl
60 dpl
G
PCs
Number of cells
Olig2+APC+ cells
Olig2+APC- cells
Distance [µm]
0-10
10-20
20-30
30-40
40-50
50-60
60-70
70-80
80-90
90-100
H
PLCs
Number of cells
Olig2+APC+ cells
Olig2+APC- cells
Distance [µm]
0-10
10-20
20-30
30-40
40-50
50-60
60-70
70-80
80-90
90-100

Figure S1

**Figure S1: ECs proliferate during remyelination, Related to Figure 1**

(A) Confocal images showing RECA-1 staining with indicated lesion area in ethidium bromide demyelinated rat CCP (5, 14, 21 dpl). (B) Graph displaying fraction of RECA-1+ area within lesion area at 5 and 21 dpl. (C) Confocal images illustrating typical RECA-1/Ki67 staining. Arrows indicate proliferating ECs (RECA-1+/Ki67+). (D) Graph showing proliferating ECs within the total EC population. Graphs display (E) total EC numbers (RECA-1+) and (F) total PC (vessel associated PDGFRb+) numbers within the lesion area, during remyelination. (G, H) Graphs displaying the frequency distribution of Olig2+APC+ and Olig2+ APC- cells and their distance to PCs and PLCs. $n \geq 3$ animals were analyzed for each condition and time point. Quantified data are represented as mean ± SEM. Data were analyzed by one-way ANOVA followed by Tukey's post hoc test, student's T test or Chi square distributions respectively $*p < 0.05$, $**p < 0.01$, $***p < 0.001$. Scale bars: (A, C) 300 µm.

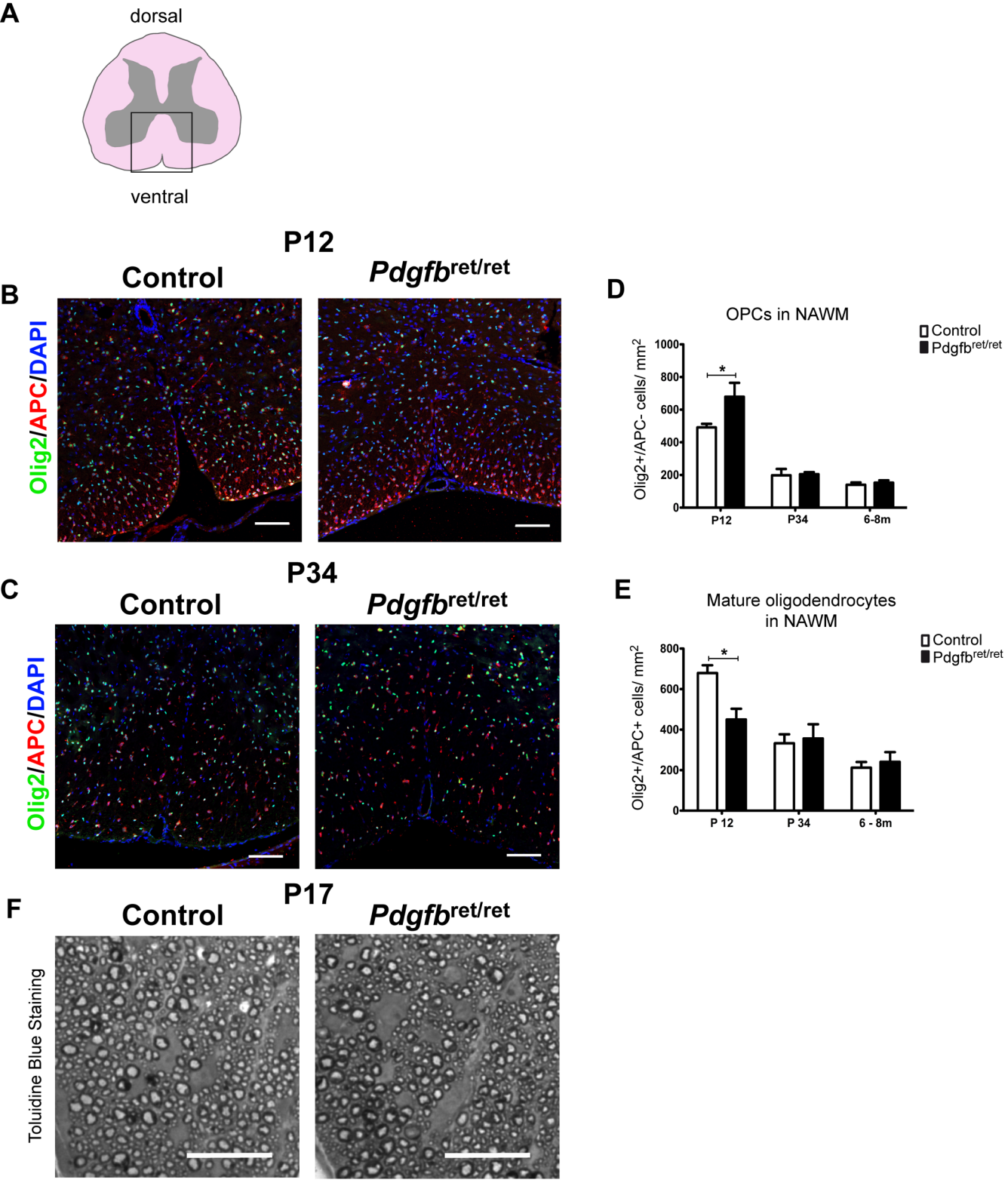
A
dorsal
ventral
P12
Control
Pdgfb ret/ret
B
Olig2/APC/DAPI
P34
Control
Pdgfb ret/ret
C
Olig2/APC/DAPI
P17
Control
Pdgfb ret/ret
F
Toluidine Blue Staining
D
OPCs in NAWM
Control
Pdgfb ret/ret
Olig2+/APC- cells/ mm2
1000
800
600
400
200
0
*
P12
P34
6-8m
E
Mature oligodendrocytes in NAWM
Control
Pdgfb ret/ret
Olig2+/APC+ cells/ mm2
800
600
400
200
0
*
P 12
P 34
6 - 8m

Figure S2

**Figure S2: Oligodendrocyte differentiation is delayed in *Pdgfb*$^{ret/ret}$ mice development, Related to Figure 2**

(A) Schematic illustration of the analyzed white matter region in the unlesioned spinal cord. (B, C) Confocal images display mature oligodendrocytes (Olig2+/APC+) in spinal cord ventral NAWM at P12 and P34. (D) Graph shows content of Olig2+/APC- cells / $mm^2$ and (E) Olig2+/APC+ cells/$mm^2$ of NAWM in P12, P34 and 6-8 months old control and *Pdgfb*$^{ret/ret}$ mice. (F) Light microscope images display myelination in the ventral spinal cord area at P17 observed by toluidine blue staining. n = 2 animals were analyzed for each condition for immunofluorescence and n=3 animals were analyzed for each condition by toluidine blue staining. Quantified data are presented as means ± SEM. Data were analyzed by two-way ANOVA followed by Bonferroni's post hoc test. *$p<0.05$. Scale bar 100 µm.

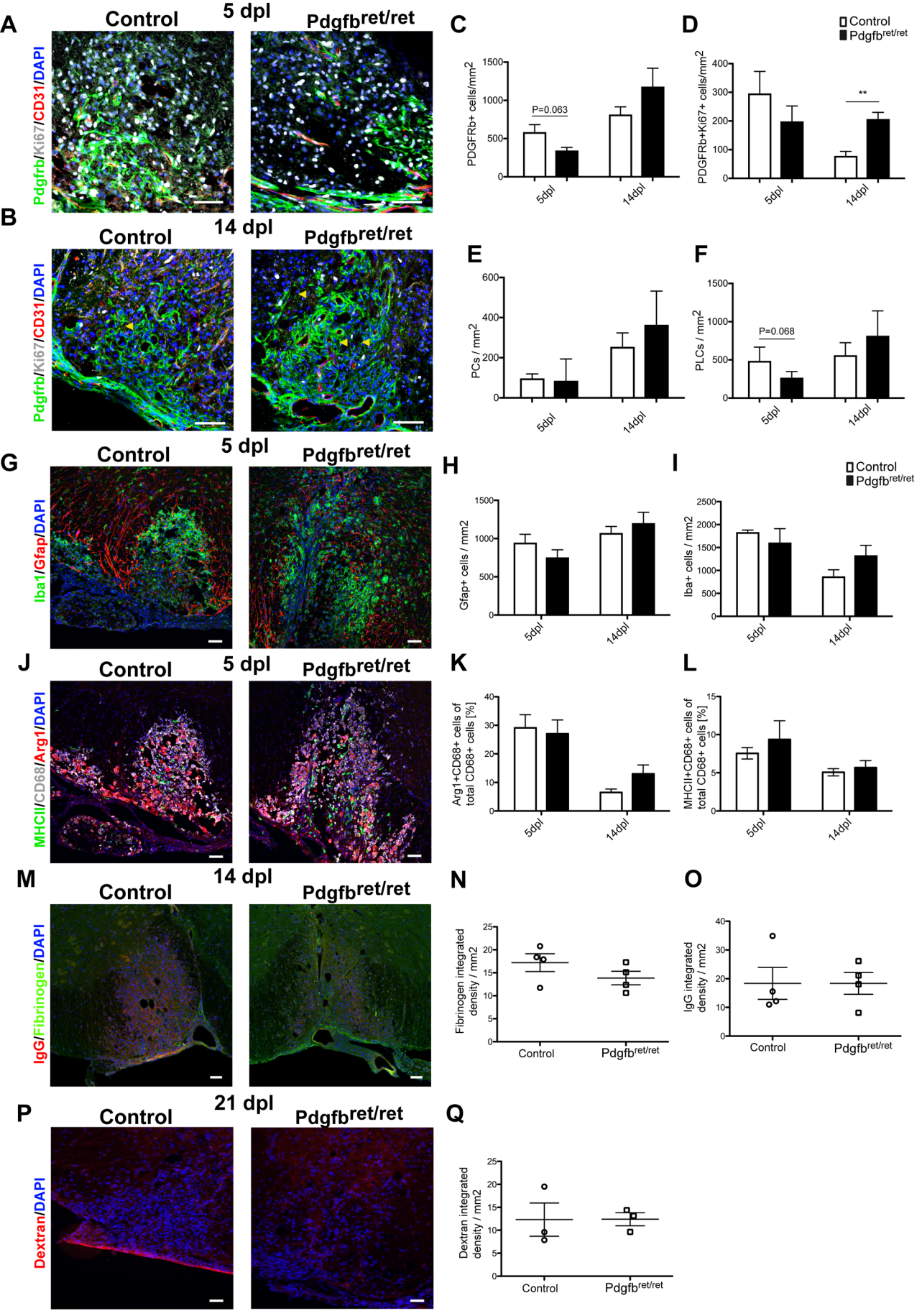
A
5 dpl
Control
Pdgfb ret/ret
Pdgfrb/Ki67/CD31/DAPI
B
14 dpl
Control
Pdgfb ret/ret
Pdgfrb/Ki67/CD31/DAPI
C
PDGFRb+ cells/mm2
P=0.063
5dpl
14dpl
D
Control
Pdgfb ret/ret
PDGFRb+Ki67+ cells/mm2
**
5dpl
14dpl
E
PCs / mm2
5dpl
14dpl
F
PLCs / mm2
P=0.068
5dpl
14dpl
G
5 dpl
Control
Pdgfb ret/ret
Iba1/Gfap/DAPI
H
Gfap+ cells / mm2
5dpl
14dpl
I
Control
Pdgfb ret/ret
Iba+ cells / mm2
5dpl
14dpl
J
5 dpl
Control
Pdgfb ret/ret
MHCII/CD68/Arg1/DAPI
K
Arg1+CD68+ cells of total CD68+ cells [%]
5dpl
14dpl
L
MHCII+CD68+ cells of total CD68+ cells [%]
5dpl
14dpl
M
14 dpl
Control
Pdgfb ret/ret
IgG/Fibrinogen/DAPI
N
Fibrinogen integrated density / mm2
Control
Pdgfb ret/ret
O
IgG integrated density / mm2
Control
Pdgfb ret/ret
P
21 dpl
Control
Pdgfb ret/ret
Dextran/DAPI
Q
Dextran integrated density / mm2
Control
Pdgfb ret/ret

Figure S3

**Figure S3: PDGFRb+ cells show a high proliferation rate in *Pdgfb*$^{ret/ret}$ mice upon lysolecithin lesion induction, Related to Figure 2**

(A, B) Confocal images show the PC and PLC distribution and proliferation in the lesion at 5 and 14dpl. (C-F) Graphs display the quantification of PDGFRb+ cells and their proliferation. PDGFRb+ cells density is lower at 5dpl but catches up at 14dpl showing a high proliferative response in the *Pdgfb*$^{ret/ret}$ mice. (G-I) Immunostaining and quantification showing astrocyte and microglia/macrophage cell marker expression in the lesion in control and *Pdgfb*$^{ret/ret}$ mice. (J-L) Confocal images and graphs showing the expression of pro-inflammatory and anti-inflammatory microglia/macrophages in the lesion of control and *Pdgfb*$^{ret/ret}$ mice. (M) Immunostaining of fibrinogen and IgG at 14dpl in control and *Pdgfb*$^{ret/ret}$ mice to determine blood brain barrier stability. (O) Graph displays quantification of fibrinogen and IgG integrate density per lesion area. (P) Images showing immunostaining for dextran extravasation at 21dpl in lesions from control and *Pdgfb*$^{ret/ret}$ mice. (Q) Graph displays the quantification on the dextran's integrated density per lesion area in control and *Pdgfb*$^{ret/ret}$ mice. n=4 mice per condition were analyzed at 5 and 14dpl and n=3 mice were analyzed at 21dpl. Quantified data are represented as means ± SEM. Data were analyzed by Students t-test or U-Mann Whitney test per time point. **p<0.01. Scale bar 50µm.

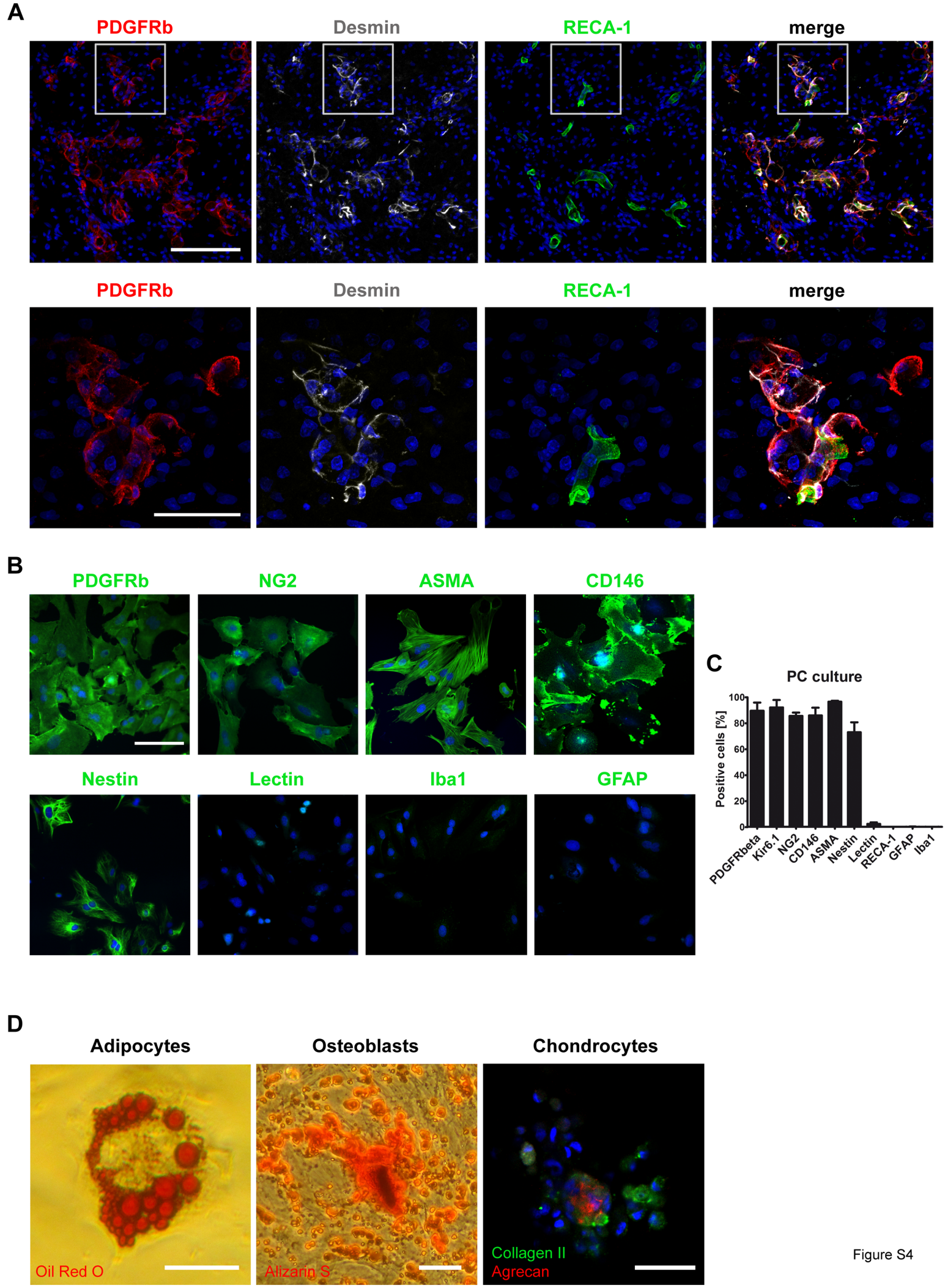
A
PDGFRb
Desmin
RECA-1
merge
PDGFRb
Desmin
RECA-1
merge
B
PDGFRb
NG2
ASMA
CD146
Nestin
Lectin
Iba1
GFAP
C
PC culture
Positive cells [%]
100
80
60
40
20
0
PDGFRbeta
Kir6.1
NG2
CD146
ASMA
Nestin
Lectin
RECA-1
GFAP
Iba1
D
Adipocytes
Osteoblasts
Chondrocytes
Oil Red O
Alizarin S
Collagen II
Agrecan

Figure S4

**Figure S4: Immunohistological characterization of PCs, Related to Figure 3**

(A) Confocal images showing expression of PDGFRb, desmin and RECA-1 in lesion area of ethidium bromide demyelinated rats (21 dpl). Boxed areas are shown in the lower panel in higher magnification. (B) Fluorescence images display cultured PCs positive for the PC-specific markers PDGFRb, NG2, ASMA, CD146, Nestin, and did not stain with Lectin, a staining indicating EC, the microglial marker Iba1 and the astrocyte marker GFAP. (C) Graph shows quantification of different markers expressed by cultured PCs. (D) Phase contrast and fluorescence images showing mesenchymal lineage differentiation potential of cultured PCs: adipocytes (Oil red O); osteoblasts (Alizarin S) and chondrocytes (Collagen II and Agrecan). Scale bars: (A) 100 μm, high magnification 20 μm, (B) 100 μm, (D) 50 μm.

## Supplementary Experimental Procedures

### Animals, surgical procedures and tissue processing

Animal experiments within this research have been regulated under the Animals (Scientific Procedures) Act 1986 Amendment Regulations 2012 following ethical review by the University of Cambridge Animal Welfare and Ethical Review Body (AWERB) in accordance with UK Home Office regulations (Project License: 70/7715) and in accordance with Austrian laws on animal experimentation and were approved by Austrian regulatory authorities (Permit No. BMWF-66.012/0001-II/3b/2014; license codes BMBF-66-012/0037-WF/V/3b/2014 and BMWF-66.012/0032-WF/V/3b/2015). During this study, 2-3 months old Sprague Dawley rats and 12 weeks old *Pdgfb*$^{ret/ret}$ mice (hetero- and homozygous), which were previously described in (Armulik et al., 2010; Lindblom et al., 2003; Nystrom et al., 2006)), were used for toxin induced demyelinations. Rats were anesthetized by inhalation of Isoflurane/Oxygen (2-2.5 $O_2$ 1000ml/min) under analgesia (Buprenorphine 0.05mg per kg body weight) and demyelinated in the caudal cerebellar peduncles by ethidium bromide local injection as previously described in (Woodruff and Franklin, 1999). Rats were sacrificed at different time points 5, 14, 21 and 60 dpl by transcardial infusion of 4% paraformaldehyde (PFA) (under terminal anaesthesia) and brains were post-fixed overnight in 4% PFA (at 4 °C). Tissue was cut on a cryostat in 12 µm slices.

Mice were anesthetized with 65 mg/kg Ketamin, 13 mg/kg Xylazin and 2 mg/kg Acepromacin by intra peritoneal injection or by inhalation of Isoflurane/Oxygen (2-2.5 $O_2$ 1000ml/min) under analgesia (Buprenorphine). Local Lysolecithin-driven demyelination in mice was induced in the ventrolateral spinal white matter as previously described in (Fancy et al., 2009). Mice were sacrificed 5dpl, 14 dpl and 21dpl by transcardial infusion of 4% PFA under terminal anesthesia and spinal cord tissue was post-fixed for 6 hrs in 4% PFA (at 4°C). Tissue was cut on a cryostat in 12 µm slices. For toluidine blue experiments mice were sacrificed at 21dpl by transcardial infusion of 4% Glutaraldehyde under terminal anesthesia and spinal cord tissue was post-fixed for 2h in 4% Glutaraldehyde (at 4°C). Tissue was embedded in resin and cut in 1µm resin sections with the microtome.

For the blood brain barrier stability experiment (Dextran extravasation measurement) 10kDA biotin conjugated Dextran molecule (Sigma Aldrich) was injected intravenously to each mice and 15min after the mice were euthanized without intracardial perfusion. Spinal cords were post- fixed in 4% PFA and then embedded in OCT for further cryostat sectioning.

### Transgenic mice

PDGF-B retention motif knock-out (*Pdgfb*$^{ret/ret}$, pericyte-deficient) and control (heterozygous littermates) mice (Lindblom et al., 2003) were used in this study either alone or crossed with Pdgfrb-eGFP mice (Gensat.org. Line name: Tg(PdgfrbeGFP)JN169Gsat/Mmucd). Pericyte-deficient mice have only 15-25% of brain capillaries covered by pericytes as compared to the control mice (Armulik et al., 2010). Animal experiments were approved by the Stockholm North Ethical Committee on Animal Research (Permit number N16/12), the Uppsala Ethical Committee on Animal Research (Permit number: C224/12 and C225/12), and by the Cantonal Veterinary Office Zurich, Switzerland (ZH196/2014).

### Preparation of primary CNS pericytes

Preparation was performed following Dore-Duffy protocol (Dore-Duffy et al., 2006) with modifications. Briefly, rat primary pericytes (PCs) were isolated from 6 – 8 weeks old female Fisher 344 rats. 5 Rats were anesthetized by Isofluran and subsequently decapitated. Brains were collected in ice-cold alphaMEM (Gibco). Meninges were removed properly and brains were minced in alphaMEM by a douncer until homogenized. Half of a centrifugation tube was filled with 4°C cold 15% dextran solution in alphaMEM (autoclaved) and carefully overlayed with brain homogenate and centrifuged at 5000 g at 4°C for 10 min. Pellet containing cerebral vessels was collected and washed once with alphaMEM (1000 g, 10 min, 4°C). Vessels were resuspended in alphaMEM and filtered through a 150µm mesh and the flow-through was again filtered through a 40 µm mesh to get rid of single cells. Microvessels were collected in alphaMEM. After centrifugation (1000g, 10 min, 4°C), microvessels were digested in a waterbath for 30 min at 37°C

with 0.01% papain (Worthington Biochemicals, England), 0.1% dispase II (Sigma), 0.01% DNase I (Worthington Biochemicals), 0.1% collagenase 1 (Life Technologies) and 12.4 mM MgSO4 in HBSS without Mg2+/Ca2+ (Life Technologies). Every 10min digested microvessels were resuspended and centrifuged (1000 g, 10 min) and the pellet collected. Cells were cultured in 1 well of a 12 well plate in alphaMEM containing 20% FBS (Gibco) and 100U/ml Penicillin/ 100µg/ml Streptomycin (Thermo Fisher) in a humidifying incubator (20% $O_2$, 5% $CO_2$ at 37°C). PCs were cultured in alphaMEM containing 20% FBS and from passage 1 they were cultured in alphaMEM containing 10% FBS. Passaging was done by 0.25% Trypsin in PBS. Passages 6-10 were used for the experiments.

**Preparation of primary bone marrow-derived mesenchymal stem cells**

Rat bone marrow-derived mesenchymal stem cells (MSCs) were prepared as previously described in (Rivera et al., 2006). Briefly, 6 – 8 weeks old female Fisher 344 rats were anesthetized by Isofluran and sacrificed. Bones were isolated from the hind limbs and bone marrow was washed out and dissociated in a petri dish using a filled syringe with alphaMEM. Bone marrow was washed twice with alphaMEM and seeded in a P100 petri dish in alphaMEM containing 100U/ml Penicillin/ 100µg/ml Streptomycin (Thermo Fisher) and 10% FBS and cultured in a humidifying incubator (20% $O_2$, 5% $CO_2$ at 37°C).

**Preparation of Oligodendrocyte Progenitor Cells**

OPCs were prepared from neonatal P0-2 Sprague Dawley rats. Rats were anesthetized with Pentobarbital and sacrificed. After removal of the hindbrain/midbrain, olfactory bulbs and meninges, cortices and hippocampi were digested with papain solution (1.2U/mL cysteine protease papain (Worthington), 3.7mg/mL DNase I type IV, 2mM L-Cysteine and 1U/mL Penicillin/ Streptomycin (Sigma Aldrich) in DMEM (Gibco). Dissociated cells were seeded in 5µg/mL poly-D-lysine coated T75 flasks. Mixed glial cultures were kept for 11DIV in medium with DMEM (Gibco), 10% fetal bovine serum (Biosera) and Mycozap PR-Plus (Lonza) prior to OPC isolation. OPCs were isolated as previously described (McCarthy and de Vellis, 1980). OPCs were seeded on 13mm coverslips in a density of 30000 cells/$cm^2$ and cultured at 37°C in 5% $CO_2$ in SATO medium (DMEM (Gibco), 1U/mL Penicillin/Streptomycin, 10 µg/mL BSA, 0.06 µg/mL progesterone, 16.1µg/mL putrescine, 0.005 µg/ mL sodium selenite, 5 µg/mL insulin and 50 µg/mL holo-transferrin (Sigma)). 10ng/mL of PDGF-AA and 10ng/mL bFGF (Preprotech) were added daily to keep cells as precursors. After 3 DIV medium was changed to PC-CM or MSC-CM. Conditioned media was replaced every 2 days and OPCs were fixed with 4% PFA at 0, 2, 4 and 6 days.

**Collection of conditioned media**

PCs and MSCs were each seeded at a cell density of 12,000 cells per $cm^2$ and incubated in the appropriate medium. After 3 days of incubation, medium was filtered using a 0.22 µm filter and kept at 4°C until use. Independent cell preparations were used for each conditioned media collection and each experiment was done with different conditioned media.

**Differentiation of pericytes**

For differentiation into adipocytes, PCs were seeded in 12 well plates and treated with AdipoLife™ DfKt-1TM Adipogenesis Medium (Lifeline Cell technology) for 2 weeks. For differentiation into osteoblasts, PCs were seeded in 6 well plates and treated with OsteoLife™ (Lifeline Cell technology) osteogenesis medium for 3 weeks. For chondrocyte differentiation, PCs were pelleted in 15 ml Falcon tubes and treated with ChondroLife™ chondrocyte differentiation medium (Lifeline Cell technology) for 3 weeks.

**Blocking of Lama2 in pericyte-derived conditioned medium**

PC-CM was collected as described above. To block Lama2 in the PC-CM, the medium was incubated with a 1:50 dilution of either general rabbit IgG antibody (Santa Cruz Biotechnologies) or rabbit anti-Lama2 antibody (Santa Cruz Biotechnologies) in rotation for 2h at room temperature and covered from light. Following incubation, the OPC medium was replaced by the PC-CM (pre-incubated with the different antibodies). This process was repeated with every medium change (at 0, 2 and 4 DIV). As a control for the effect of the antibodies in OPCs, the pre- incubation with the corresponding antibodies was also performed for the control unconditioned medium in parallel.

PCs were trypsinized from 10cm dishes, counted and seeded at a density of 75000 cells per 12 well. The following day media was changed to basic OPC control media without P/S and the next morning PCs were transfected using Lipofectamine siRNA max. PCs were transfected using Opti-Mem (Gibco), 2.5µl Lipofectmine RNAi max (Invitrogen) and 50nM of non-targeting or rat –Lama2 siRNA (Dharmacon) per 12 well. After 6h media with transfections reagents was removed and fresh OPC control media added. OPC control media was incubate for 48h with the transfected PCs and then collected and filtered through a 0.22µm filter prior to its addition to OPCs.

**Demyelination of organotypic slices**

Remyelination of rat cerebellar slices was prepared as previously described (Birgbauer et al., 2004). Briefly, P9 Sprague Dawley rats were euthanized by overdose of anesthetic and the cerebellum was cut in 300 µm thick sagittal slices using a McIllwain Tissue chopper. Slices were incubated on 4.0µm pore 30mm diameter filter (Millipore) for 7 DIV in organotypic slice medium (50% basal Eagle medium (BME) (Gibco), 25% heat inactivated horse serum (Gibco), 25% HBSS (BME) (Gibco), 5mg/mL glucose, 1X Glutamax (Gibco) and 1X Mycozap – PR plus (Lonza)), with medium changes every other day. After 7 DIV, medium was replaced by organotypic slice medium containing 0.5mg/mL lysolecithin for 16h. After 16h medium was replaced by PC conditioned organotypic slice medium and non-conditioned control medium. Medium was replaced by new PC-CM every other day and slices were fixed at 0dpl, 2dpl, 4dpl, 6dpl and 8dpl with 4% PFA for 1h at room temperature. Slices stored at -20°C in PBS until immunostaining was performed. Independent slice culture preparations were used to generate the data.

**Immunocytochemistry**

**Pericytes**

PCs and MSCs were detached by 0.25% Trypsin and seeded on uncoated glass coverslips at a density of $1\times10^4$ cells/$cm^2$. Cells were fixed with 4% paraformaldehyde (PFA) with pH 7.4 for 10 - 15 min and washed 3x with phosphate buffered saline (PBS). Cells were blocked with fish skin gelatin buffer (FSGB) containing TBS (0.15 M NaCl, 0.1 M Tris-HCl, pH 7.5), 0.1% Triton-X100 (only for intracellular antigens), 1% bovine serum albumine (BSA) and 0.2% Teleostean gelatin (Sigma, Germany) for 2hrs at room temperature (RT). Primary antibodies were applied in blocking solution overnight at 4°C. Cells were incubated with fluorochrome-conjugated species-specific secondary antibodies at RT for 2hrs and washed 3x with PBS. To analyze the marker expression profile the following antibodies were used. Primary antibodies: rabbit anti-glial fibrillary acidic protein (GFAP) 1:1000 (Dako); mouse anti-rat Nestin 1:500 (BD Pharmingen); rabbit anti-NG2 1:200 (Millipore); goat anti platelet-derived growth factor receptor beta (PDGFRb) 1:100 (R & D Systems); rabbit anti Kir 6.1 1:100 (Abcam); mouse anti CD146 (MUC18) 1:100 (Invitrogen); mouse anti alpha smooth muscle actin (ASMA) 1:500 (Sigma); rabbit anti Iba1 1:300 (Wako); biotinylated Lectin from *B. simplicifolia* (1:500, Sigma-Aldrich); mouse anti RECA-1 1:500 (Abcam); rabbit anti Desmin 1:200 (Abcam). Secondary antibodies: donkey anti-rabbit conjugated with Alexa 568 1:1000 (Invitrogen); donkey anti-rabbit conjugated with Alexa 488 1:1000 (Invitrogen); donkey anti-rabbit conjugated with Alexa 647 1:1000 (Millipore); donkey anti-goat conjugated with Alexa 488 1:1000 (Invitrogen); donkey anti-goat conjugated with Alex 568 1:100 (Invitrogen); donkey anti-mouse conjugated with Alexa 488 1:1000 (Invitrogen); donkey anti-mouse

conjugated with Alexa 568 1:1000 (Invitrogen); donkey anti-mouse conjugated with Cy5 1:1000 (Jackson); Streptavidin conjugated with Alexa 488 1:500 (Invitrogen); Streptavidin conjugated with Alexa 568 1:500 (Invitrogen, Austria). For the detergent-sensitive antigens (i.e. NG2) Triton X- 100 was omitted from FSGB. Nuclear counterstaining was performed with 4´, 6´-diamidino-2-phenylindole dihydrochloride hydrate 0.25 µg/µl (DAPI; Sigma). Specimens were mounted on microscope slides using Prolong Antifade kit (Molecular Probes).

**Oligodendroglial progenitor cells**

OPCs were fixed in 4% PFA (pH 7.4) for 10 – 15min and washed twice with PBS for 10 min. Cells were blocked with 5% normal donkey serum (NDS) (Sigma Aldrich) and 0.1% Triton for 1 h at RT. Primary antibodies were applied in 5% NDS and 0.1% Triton over night at 4 °C. Cells were washed and incubated in 5% NDS with fluorochrome-conjugated species-specific secondary antibodies at RT for 2hrs and washed 3x with PBS. To analyze the marker expression profile the following antibodies were used. Primary antibodies: goat anti-Olig2 1:200 (R and D Systems), rabbit anti- Olig2 1:500 (Millipore), mouse anti-2`, 3`-cyclic-nucleotide-3`- phosphodieesterase (CNP) 1:400 (Abcam), rat anti-myelin basic protein (MBP) 1:500 (Serotec), mouse anti- NG2 1:200 (Millipore), rabbit anti-Ki67 1:500 (Abcam) and rabbit anti-active caspase 3, 1:500 (Millipore). Secondary antibodies: donkey anti-rabbit conjugated with alexa 488; donkey anti-mouse conjugated with alexa 647; donkey anti-goat conjugated with alexa 488 and donkey anti-rat conjugated with alexa 568. All secondary antibodies were diluted 1:500 and they were purchased from Invitrogen. Specimens were mounted on microscope slides using fluoromount G (Southern Biotech).

**Immunohistochemistry**

**Cryo sections**

For Figures 1, 2, S1, S2, S3 and S4: Immunohistochemistry was performed as previously described in Kazanis et al 2015 (Kazanis et al., 2015). Briefly, cryo sections were warmed to room temperature and rehydrated in PBS. Antigen retrieval was performed with boiled citrate buffer (Sigma) for 10 min and washed 3x 10 min with PBS. Sections were blocked with 10% normal goat or donkey serum and 0.1% triton and incubated with antibodies in appropriate dilutions, washed and mounted with Fluoromount G (Southern Biotech). Primary antibodies: goat anti platelet-derived growth factor receptor beta (PDGFRb) 1:100 (R & D Systems); rabbit anti Desmin 1:200 (Abcam); mouse anti RECA-1 1:500 (Abcam); rabbit anti Olig2 1:300 (Millipore); Mouse anti CC1 1:500 (Calbiochem); rabbit anti Ki67 1:100 (Thermo Scientific); rabbit Ki67 (Abcam), rat anti CD31 (BD Pharmingen); rabbit anti Laminin 1:300 (Sigma Aldrich); rabbit anti CD68 1:500 (Abcam), rat anti MHCII 1:100 (eBiosciences); goat anti Arginase I 1:100 (Santa Cruz Biotechnologies); goat anti Iba1 1:500 (Abcam); chicken anti GFAP 1:1000 (Abcam) and sheep anti fibrinogen 1:200 (Bio-Rad). Stainings of APC on mouse tissue was performed using Mouse On Mouse basic kit (Vector labs). Secondary antibodies: donkey anti-rabbit conjugated with Alexa 568 1:1000 (Invitrogen); donkey anti-rabbit conjugated with Alexa 488 1:1000 (Invitrogen); donkey anti-rabbit conjugated with Alexa 647 1:1000 (Millipore); donkey anti-goat conjugated with Alexa 488 1:1000 (Invitrogen); donkey anti-goat conjugated with Alex 568 1:100 (Invitrogen); donkey anti-mouse conjugated with Alexa 488 1:1000 (Invitrogen); donkey anti-mouse conjugated with Alexa 568 1:1000 (Invitrogen); donkey anti-mouse conjugated with Cy5 1:1000 (Jackson); donkey anti-chicken Alexa 594 (Invitrogen), Streptavidin conjugated with Alexa 488 1:500 (Invitrogen); Streptavidin conjugated with Alexa 568 1:500 (Invitrogen, Austria). For APC stainings, donkey anti Mouse IgG2b Alexa 647 or Alexa 488 was used. Nuclear counterstaining was performed with Hoechst (Sigma).

For Figure 4: immunohistochemistry was carried out on vibratome cut sagittal sections (50µm). Tissues were blocked and permeabilized in PBS containing 2.5% donkey serum, 1% bovine serum albumin and 0.5% TritonX-100 in PBS overnight at 4 °C. Tissues were then incubated in primary antibody solution for 48 hours at 4 °C, washed, and subsequently incubated in secondary antibody solution over night at 4 °C. Sections were mounted in Prolong Gold Antifade (Life Technologies). The following primary antibodies were used: goat anti- mouse CD31 (R&D Systems); rabbit anti-desmin (Abcam); rat anti-laminin alpha2 (Abcam). The fluorescently labeled secondary antibodies made in donkey were purchased from Jackson Immunoresearch.

**Organotypic Slices**

For immunostaining, slices were blocked for 1h with 10% normal goat serum 0.5% Triton X-100 in agitation and incubated overnight with primary antibodies in blocking solution. Slices were washed three times with PBS 0.1% Triton X-100 and then incubated with secondary antibodies for 2h at room temperature. The secondary antibodies were removed washing with PBS 0.1% Triton X-100 and then Hoechst (1µg/mL final concentration, Sigma) was used for nuclei staining. Slices were mounted with Fluoromount G onto poly D- lysine slides and covered with a 20mm coverslip (VWR). Primary antibodies: rat anti-myelin basic protein (MBP) 1:500 (Serotec) and rabbit anti- neurofilament H 1:500, (Abcam). Secondary antibodies: goat anti-rabbit conjugated with Alexa 488, 1:500, (Invitrogen) and goat anti-rat conjugated with Alexa 568 1:500 (Invitrogen).

**Developmental myelination and remyelination assessment**

Microtome cut 21dpl 1µm slices were stained in a heat plate with Toluidine Blue and the excess of toluidine blue was washed out with MiliQ water and images were taken with light microscopy. For remyelination the different lesions were blindly ranked. Two independent people organized and ranked them according to their level of demyelination and remyelination.

**In situ hybridization**

The expression of a number of marker mRNA species in demyelinated lesions was examined by *in situ* hybridization with digoxigenin-labelled cRNA probe for *Plp*. Animals were perfused with 4% PFA via the left heart ventricle. The tissue was extracted, post-fixed in 4% PFA overnight at 4ºC and cryoprotected in 20% sucrose. *In situ* hybridizations were conducted on cryostat sections (12 µm) using previously established protocols (Kotter et al., 2006; Zhao et al., 2008).

**Fluorescence *in situ* hybridization**

In situ RNA hybridization was performed using RNAscope technology (Advanced Cell Diagnostics) following the manufacturer's protocol with minor modifications. Briefly, fresh-frozen brains from 2-month old mice were cut into 16 µm sagittal sections and mounted on SuperFrost Plus glass slides. After dehydration, slides were subjected to RNAscope Multiplex Fluorescent Assay. First, slides were incubated in Pretreat 4 for 20 min at RT. After that, RNAscope probes were hybridized for 2 h at 40 °C and the remainder of the assay protocol was implemented. The fluorescent signal emanating from RNA probes was visualized and captured using a Leica TCS SP8 confocal microscope (Leica Microsystems). Images are presented as 2D maximum intensity projections of ~3 µm z-stacks. According to the Advanced Cell Diagnostics, each mRNA molecule hybridized to a probe appears as a separate small fluorescent dot.

**Lama2 mRNA expression by Affymetrix and RNAseq**

The Affymetrix array data were downloaded from NCBI GEO database (accession number: GSE15892) published by Armulik et al. (Armulik et al., 2010). The raw Affymetrix data were normalized using Bioconductor GCRMA package (Bioconductor gcrma package, version 2.32.0), and Significance Analysis of Microarrays was performed to identify the significantly differentially expressed genes (Bioconductor Siggenes package, version 1.34.0). Also RNAseq data of Lama2 expression in sorted pericytes vs. microvascular fragments was extracted from our previous publication (He et al., 2016).

**Western Blot**

Proteins were isolated from rat cerebellum in liquid nitrogen frozen, dissociated with a mortar and resuspended in RIPA buffer. *In vitro* cultured PCs were harvested with a cell scraper and resuspended in RIPA. Tissue and cells were homogenized and after 30 min incubation at 4 °C, lysate was spun at 13000 rpm for 15 min, protein concentration of supernatant was measured using Pierce BCA Protein Assay Kit (Thermo Fisher). 3x 4ml PC- CM and control medium was filtered through a 5kDa Amicon Ultra centrifugal filter unit (4000g, 4°C in a swinging rotor). Western blot was performed using Bio-Rad Mini-PROTEAN® TGX Stain-Free™ Precast gradient gels in a Bio-Rad wet chamber. 10 µg of protein sample and total amount of filtrate was loaded after adding Laemmli (95°C 5min) and run with 120 V. Precision Plus Protein™ Dual Color Standard (Bio-Rad) as well as SeeBlue® Plus2 Pre-stained Protein Standard (Thermo Fisher). Blotting was performed using a Trans- Blot® Turbo™ Transfer System (Bio-Rad) with Trans-Blot® Turbo™ Mini PVDF Transfer Packs (Bio-Rad). Membranes were blocked with 5% BSA in tris buffered saline with 0.1% Triton (TBST) for 1 h at room temperature following primary antibody incubation over night at room temperature (rabbit anti Lama2 1:200 (Santa Cruz); mouse anti beta Actin 1:2000 (SIGMA), washed with TBST and incubated with secondary antibodies in blocking solution for 2 hrs at room temperature (donkey anti rabbit Alexa 488 1:1000 (Invitrogen); donkey anti mouse Alexa 568 1:1000 (Invitrogen)). Antibody-labeled proteins were visualized using Chemidoc (Bio-Rad).

**Histological analyses**

As all caudal cerebellar peduncle (CCP) lesions have been performed in both hemispheres, analyses were carried out in both lesions and rostral, central and caudal regions were taken into consideration to determine a mean value (cell quantification within lesion area, 2 lesions per animal and different layers of lesion) per animal. Similarly, mean values were determined for ventral spinal cord WM lesions. All cellular quantifications were performed within a defined NAWM (CCP/ ventral spinal cord WM) region or within a lesion area in the respective WM. Lesions were recognized by hypercellularity indicated by DAPI signal. Lesions affecting the neighboring grey matter were excluded from analyses.

Lysolecithin lesions were recognized by its hypercellularity indicated by DAPI signal and images containing the full lesion of at least three section of each animal were acquired by microscopy using Z-Stack. For quantification of the different cells a maximum projection of the confocal stacks was created using Fiji and the different cell types quantified either manually using Cell Counter or using colocalization masks macros in Fiji.

For immunocytochemistry at least 5 fields selected by DAPI were imaged per condition using confocal microscopy stacks. Then using Fiji a maximum projection of each the confocal stacks was created and the different cell types quantified either manually using Cell Counter or using colocalization masks macros in Fiji.

**Quantification of PCs and ECs**

For quantifications of PCs and ECs, immunohistochemistry against PDGFRb and RECA-1, respectively, counterstained with DAPI was carried out, followed by confocal imaging (z-stacks of 12µm slices and 40x magnification) and analyzed using ImageJ. Only vessel-associated cells displaying processes extending along microvessels, a clear roundish nucleus and PDGFRb expression have been considered as PCs. ECs have been quantified following criteria such as a clear RECA-1 staining and a clearly visible cigar-shaped or elongated nucleus (within the microvasculature). A PDGFRb or RECA-1 staining without nucleus (or without a clearly identifiable round/cigar-shaped or elongated nucleus) has not been taken into consideration. Quantification of PLCs followed the same basic criteria, such as a clear PDGFRb staining as well as clear round nucleus. These cells in turn, were counted as PLCs only if their processes were completely detached from vessels. PLCs were not considered when a RECA-1 signal (even if without nucleus) was found in close vicinity. Following these criteria the EC:PC ratio was determined upon quantification of EC and PC total numbers within the same area.

**Cell distance measurements**

We analyzed the CCP / ventral spinal cord WM lesions at 14dpl. To evaluate the distance between Olig2+ cells and RECA-1+ or PDGFRb+ cells, we used Z-stack confocal images taken of demyelination lesions (12µm slices), as described above. Measurements were performed using ImageJ distance tool. Only PCs and ECs with visible nucleus and clear staining were considered. Only the shortest distance starting from each Olig2-expressing nucleus present within the lesion to the edge of the respective closest RECA-1 or PDGFRb signal was determined. Similarly, as described above, mean values have been determined per animal.

To analyze maturation of oligodendrocytes (Olig2 and APC) and its proximity to PDGFRb+ cells, we performed PDGFRb/Olig2/APC/RECA1 stainings. Distance from an Olig2+ cells in straight line to the center of the closest PDGFRb+ cells was measured. Then both cells were analyzed to observed if the cells were APC+ or APC- and if the PCs were attached to blood vessels (PCs) or not (PLCs). Based on these criteria, we created a plot with the averaged frequency within the three animals and created a frequency distribution for Olig2+ APC- and Olig2+ APC+ cells.

**Statistical analyses**

Graphs show mean values ± SEM and statistical analysis have been performed using GraphPad Prism 5.0 (GraphPad Software Inc.) and SPSS 20 (IBM). P values below 0.05 were considered to be significant after parametric one-way ANOVA- Tukey post hoc analyses, Student t-Test or U-Mann Whitney tests (when not normally distributed). For statistical analysis with two parameters, such as time course experiments with different treatments, two-way ANOVA-Bonferroni post hoc was used. In the case of positive interaction between the two parameters, as it masks the potential differences between groups, the time parameter was separated and each of the time points analyzed individually as a two-group one parameter using either Student t-test or U-Mann Whitney. For statistical analyses comparing one parameter between only two groups, two-tailed Student's t test or U-Mann Whitney has been performed. For distance frequency distribution analysis Chi square test was used (Figure1M and S1G, H). All experiments were performed the n number indicated in the figure legend. Significance was *<0.05 **<0.01 and ***<0.001.

## Supplemental References


Armulik, A., Genove, G., Mae, M., Nisancioglu, M.H., Wallgard, E., Niaudet, C., He, L., Norlin, J., Lindblom, P., Strittmatter, K., et al. (2010). Pericytes regulate the blood-brain barrier. Nature 468, 557-561.

Birgbauer, E., Rao, T.S., and Webb, M. (2004). Lysolecithin induces demyelination in vitro in a cerebellar slice culture system. Journal of Neuroscience Research 78, 157-166.

Dore-Duffy, P., Katychev, A., Wang, X., and Van Buren, E. (2006). CNS microvascular pericytes exhibit multipotential stem cell activity. Journal of cerebral blood flow and metabolism: official journal of the International Society of Cerebral Blood Flow and Metabolism *26*, 613-624.

Fancy, S.P., Baranzini, S.E., Zhao, C., Yuk, D.I., Irvine, K.A., Kaing, S., Sanai, N., Franklin, R.J., and Rowitch, D.H. (2009). Dysregulation of the Wnt pathway inhibits timely myelination and remyelination in the mammalian CNS. Genes & development *23*, 1571-1585.

He, L., Vanlandewijck, M., Raschperger, E., Andaloussi Mae, M., Jung, B., Lebouvier, T., Ando, K., Hofmann, J., Keller, A., and Betsholtz, C. (2016). Analysis of the brain mural cell transcriptome. Scientific reports *6*, 35108.

Kazanis, I., Feichtner, M., Lange, S., Rotheneichner, P., Hainzl, S., Oller, M., Schallmoser, K., Rohde, E., Reitsamer, H.A., Couillard-Despres, S*., et al.* (2015). Lesion-Induced Accumulation of Platelets Promotes Survival of Adult Neural Stem / Progenitor Cells. Experimental neurology *269*, 75-89.

Kotter, M.R., Li, W.W., Zhao, C., and Franklin, R.J. (2006). Myelin impairs CNS remyelination by inhibiting oligodendrocyte precursor cell differentiation. The Journal of neuroscience: the official journal of the Society for Neuroscience *26*, 328-332.

Lindblom, P., Gerhardt, H., Liebner, S., Abramsson, A., Enge, M., Hellstrom, M., Backstrom, G., Fredriksson, S., Landegren, U., Nystrom, H.C., et al. (2003). Endothelial PDGF-B retention is required for proper investment of pericytes in the microvessel wall. Genes & Development 17, 1835-1840.

McCarthy, K.D., and de Vellis, J. (1980). Preparation of separate astroglial and oligodendroglial cell cultures from rat cerebral tissue. The Journal of cell biology *85*, 890-902.

Nystrom, H.C., Lindblom, P., Wickman, A., Andersson, I., Norlin, J., Faldt, J., Lindahl, P., Skott, O., Bjarnegard, M., Fitzgerald, S.M., et al. (2006). Platelet-derived growth factor B retention is essential for development of normal structure and function of conduit vessels and capillaries. Cardiovascular research 71, 557-565.

Rivera, F.J., Couillard-Despres, S., Pedre, X., Ploetz, S., Caioni, M., Lois, C., Bogdahn, U., and Aigner, L. (2006). Mesenchymal stem cells instruct oligodendrogenic fate decision on adult neural stem cells. Stem Cells 24, 2209-2219.

Woodruff, R.H., and Franklin, R.J. (1999). Demyelination and remyelination of the caudal cerebellar peduncle of adult rats following stereotaxic injections of lysolecithin, ethidium bromide, and complement/anti- galactocerebroside: a comparative study. Glia *25*, 216-228.

Zhao, C., Fancy, S.P., ffrench-Constant, C., and Franklin, R.J. (2008). Osteopontin is extensively expressed by macrophages following CNS demyelination but has a redundant role in remyelination. Neurobiology of disease *31*, 209-217.